Texture Analysis for Classification of SAR Images

Thesis submitted in partial fulfillment of the requirement for the award of degree of

Master of Engineering
in
Electronics Instrumentation and Control

By:
Gunjit Kaur
(800851007)

Under the supervision of:
Mr. M.D. Singh
Assistant Professor
EIED

JULY 2010

ELECTRICAL AND INSTRUMENTATION ENGINEERING DEPARTMENT
THAPAR UNIVERSITY
PATIALA – 147004

Declaration

*I hereby declare that the report entitled "**Texture Analysis for Classification of SAR Images**" is an authentic record of my own work carried out as requirements for the award of degree of M.E. (Electronic Instrumentation & Control) at Thapar University, Patiala, under the guidance of Mr. M.D.Singh (Assistant Professor, EIED) during January to July 2010.*

Gunjit Kaur

Gunjit Kaur

Roll. No. 800851007

Date: 30-06-10

It is certified that the above statement made by the student is correct to the best of my knowledge and belief.

(----------)

Mr. M.D. Singh

Assistant Professor, EIED

Thapar University, Patiala.

S. Ghosh 12/7/10

(----------)

Dr. Smarajit Ghosh

Professor & Head, EIED

Thapar University, Patiala.

RK Sharma 14-7-10

(----------)

Dr. R. K. Sharma

Dean of Academic Affairs

Thapar University, Patiala.

20/08/10

Dr. Savita Gupta

Professor (CSE)

PU, Chd.

Acknowledgment

The real spirit of achieving a goal is through the way of excellence and austere discipline. I would have never succeeded in completing my task without the cooperation, encouragement and help provided to me by various personalities.

With deep sense of gratitude I express my sincere thanks to my esteemed and worthy supervisor, Mr. M.D.Singh, Assistant Professor, Department of Electrical & Instrumentation Engineering, Thapar University, Patiala, for his valuable guidance in carrying out this work under his effective supervision, encouragement, enlightenment and cooperation.

I shall be failing in my duties if I do not express my deep sense of gratitude towards Mr. Smarajit Ghosh, Professor & Head of the Department of Electrical & Instrumentation Engineering, Thapar University, Patiala who has been a constant source of inspiration for me throughout this work.

I am also thankful to all the staff members of the Department for their full cooperation and help.

My greatest thanks are to all who wished me success especially my parents. Above all I render my gratitude to the ALMIGHTY who bestowed self-confidence, ability and strength in me to complete this work.

Gunjit kaur

Place: Thapar University, Patiala *Gunjit Kaur*

Date: 30-06-10

Table of contents

Abstract

SAR (Synthetic Aperture Radar) image classification has been a constant field of research since long. SAR image classification has numerous applications like map updating, oil spill detection in oceans, automatic target recognition etc. A lot of work has been done on use of Texture features, frequency spectrum features etc. for SAR image classification. But still there is scope for a simple but effective classification technique. In the present work, we have proposed a classification system for SAR images based on the highly discriminative texture features. We have studied 30 SAR images for 20 texture features. Statistical Approach has been used for texture analysis of the images. Finally, we have reduced the required number of texture features to a lesser number of features. The results being obtained are tested on test images to give an accuracy of 95% for image classification.

Organization of Thesis

The first chapter introduces the Synthetic Aperture Radar (SAR) system.

The second chapter reviews the work that has been already carried out in this field and formulation of the problem.

The third chapter discussed the Texture Analysis Models and the approach being used.

The fourth chapter gives the detailed description of methodology used to carry out the whole work.

The fifth chapter shows the results obtained in the tabular form and discussion over the result.

In the sixth chapter thesis concluded with future scopes.

List of Figures

List of Tables

List of abbreviations

SAR – Synthetic Aperture Radar

ATR – Automatic Target Recognition

EM – Electromagnetic

RF – Radio Frequency

GLCM – Gray Level Co-Occurrence Matrix

GLRLM – Gray Level Run Length Matrix

PCA – Principal Component Analysis

MRF – Markov Random Field

ASM – Angular Second Moment

IDM – Inverse Difference Moment

ARL – Average Gray Run-Length

SRE – Short Run Emphasis

LRE – Long Run Emphasis

GLN – Gray Level Non-Uniformity

RLN – Run Length Non-Uniformity

RP – Run Percentage

LGRE – Low Gray Level Run Emphasis

HGRE – High Gray Level Run Emphasis

RGB – Red Green Blue

MATLAB – Matrix Laboratory

CON – Contrast

CORR – Correlation

D_ENT – Difference Entropy

D_VAR – Difference Variance

ENT – Entropy

IMCORR1 – Information measure of Correlation 1

IMCORR2 – Information measure of Correlation 2

S_ENT – Sum Entropy

S_AVG – Sum Average

S_VAR – Sum Variance

VAR – Variance

TP – True Positive

FP – False Positive

FN – False Negative

TN – True Negative

Chapter 1
INTRODUCTION

In today's era, images are being analysed in a number of research works. These images can be medical images, synthetic aperture radar (SAR) images, and industrial images and so on. In the present work, SAR image classification is the problem in question. This field is not a novel area of research; many researchers have already explored this area. SAR image classification has been used in numerous applications like map updating, urban area classification and classification of extremely randomized clustering forests, Automatic Target Recognition (ATR) and a list to mention. In case of SAR images, texture and intensity are two important parameters on the basis of which different images can be classified. Texture holds very useful information in SAR image classification. SAR images contain some inherent echo noise called speckle, so they need special methods to characterize them. There are different approaches which can be used to identify texture patterns in a given image. For efficient classification of water cover or land cover or urban area coverage, textural measures have to be chosen suitably. In this work, Texture analysis of SAR images is being done in order to classify them as water or urban area.

1.1 SYNTHETIC APERTURE RADAR (SAR)

Synthetic-aperture radar (SAR) is a form of radar in which multiple radar images are processed to yield higher-resolution images. Either a single antenna mounted on a moving platform (such as an airplane or spacecraft) is used to illuminate a target scene or many low-directivity small stationary antennae are scattered over an area near the target area. The many echo waveforms received at the different antenna positions are post-processed to resolve the target. SAR can only be implemented by moving one or more antennae over relatively immobile targets or by placing multiple stationary antennae over a relatively large area or combinations thereof. SAR has seen wide applications in remote sensing and mapping. Since SAR is an active sensor, which provides its own source of illumination, it can therefore operate day or night. SAR has been shown to be very useful over a wide range of applications, including sea and ice monitoring, mining, oil pollution monitoring, oceanography, snow monitoring, classification of earth terrain etc.

Synthetic Aperture Radar was invented by Carl A. Wiley, a mathematician at Goodyear Aircraft Corporation in Litchfield Park, Arizona, in June 1951 while working on a correlation guidance system for the *Atlas* ICBM program. In early 1952, Wiley, together with Fred Heisley and Bill Welty, constructed a concept validation system known as DOUSER.

1.1.1 INTRODUCTION

RADAR is an acronym for Radio Detection and Ranging. Radar works like a flash camera but at radio frequency. Typical radar system consists of transmitter, switch, antenna, receiver and data recorder. The transmitter generates a high power of electromagnetic wave at radio wavelengths. The switch directed the pulse to antenna and returned echo to receiver. The antenna transmitted the EM pulse towards the area to be imaged and collects returned echoes. The returned signal is converted to digital number by the receiver and the function of the data recorder is to store data values for later processing and display. Fig. 1.1 shows the simple block diagram of a radar system. [1]

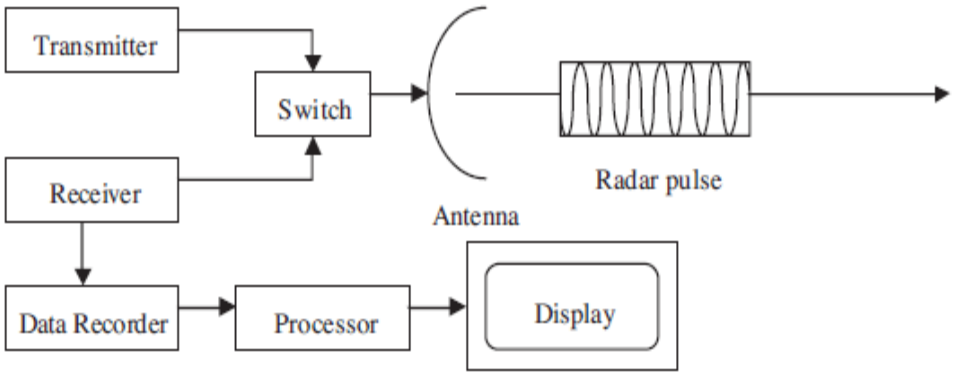

Figure 1.1 Basic block diagram of typical radar system.

The radar platform flies along the track direction at constant velocity. For real array imaging radar, its long antenna produces a fan beam illuminating the ground below. The along track resolution is determined by the beam width while the across resolution is determined by the pulse length. The larger the antenna, the finer the detail the radar can resolve. In SAR, forward motion of actual antenna is used to 'synthesize' a very long antenna. At each position a pulse is transmitted, the return echoes pass through the receiver and recorded in an 'echo store'. The Doppler frequency variation for each point on the ground is unique signature. SAR processing

involves matching the Doppler frequency variations and demodulating by adjusting the frequency variation in the return echoes from each point on the ground. Result of this matched filter is a high-resolution image. Figure below shows the synthetic aperture length.

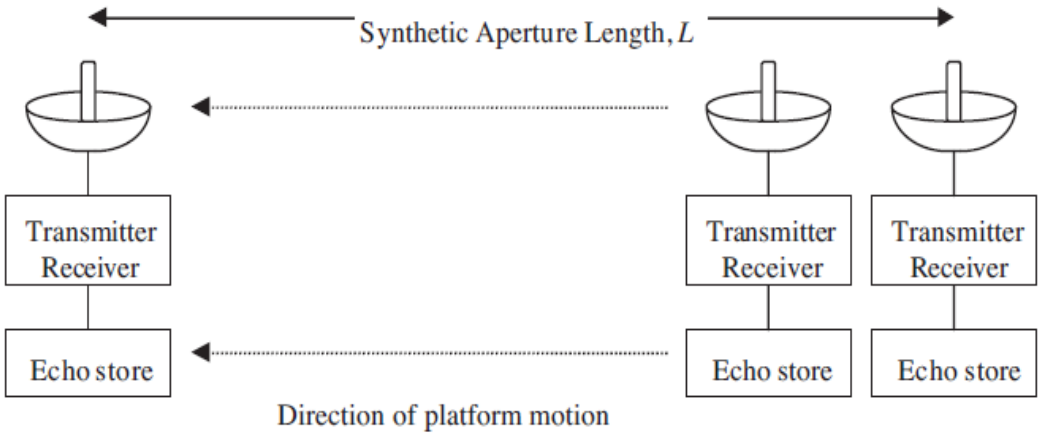

Figure 1.2 Synthetic aperture

1.2 The Description of Imaging Radar

The geometry of imaging radar is shown in Fig. 1.3. The physical aperture of the radar with width W_a and length ℓ generates a RF beam whose angular across track 3dB beam width of antenna and angular along-track 3 dB beam width of antenna is θ_V and θ_H respectively. θ_V is determined by the width and length of antenna, and wavelength of transmitted signal (λ). This relation is written as

$$\theta_V = \lambda / W_a$$

The antenna is mounted on a platform such as an aircraft that travels along a flight path with velocity v. It illuminates the shaded path (known as footprint) on the ground as the aircraft moves in the direction of flight path. The width of the ground swath is simply given by

$$W_g = \frac{\lambda R}{W_a \cos\theta}$$

where θ is the incidence angle (look angle) of the beam, R is the slant range from the antenna to the midpoint of swath. The RF energy transmitted from antenna has a duration τ_p and is repeated at a given interval, pulse repetition interval (PRI) that can be inverted to obtain the pulse repetition frequency (PRF).

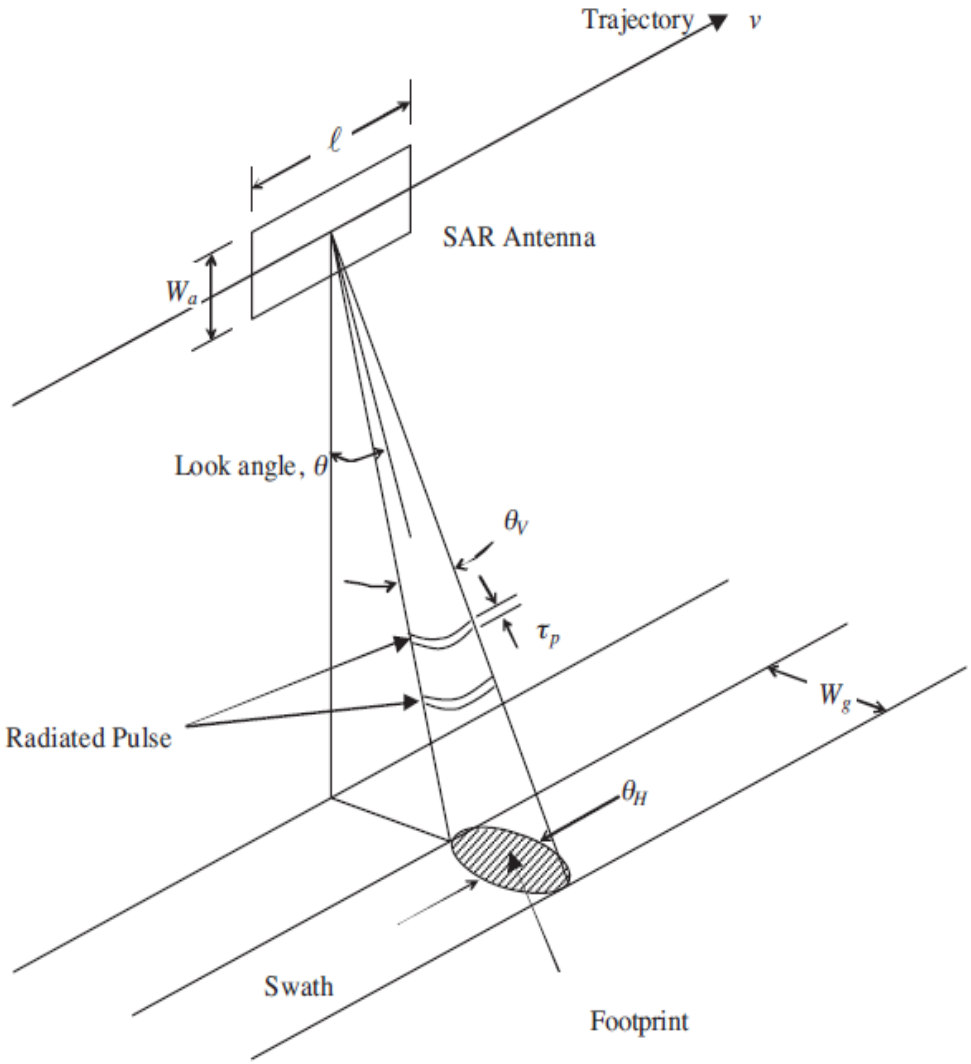

Figure 1.3 the imaging radar geometry.

1.3 SAR System

Main parts of a SAR system are depicted in Figure 1.4. A pulse generation unit creates pulses with a bandwidth according to the aspired range resolution. They are amplified by the sender and are transferred to the antenna via a circulator. The receiver gets the antenna output signal (echoes of the scene) amplifies them to an appropriate level and applies a band pass filter. After the demodulation and A/D conversion of the signals the SAR processor starts to calculate the SAR image. Additional motion information will be provided by a motion measurement system. A radar control unit arranges the operation sequence, particularly the time schedule.

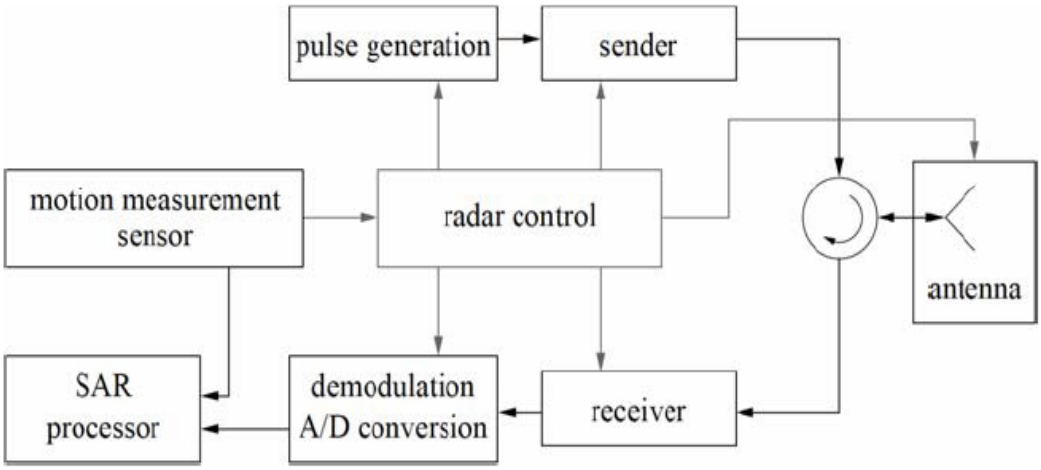

Figure 1.4 General Structure of a SAR System.

In synthetic aperture radar (SAR) imaging, microwave pulses are transmitted by an antenna towards the earth surface. The microwave energy scattered back to the spacecraft is measured. The SAR makes use of the radar principle to form an image by utilising the time delay of the backscattered signals.

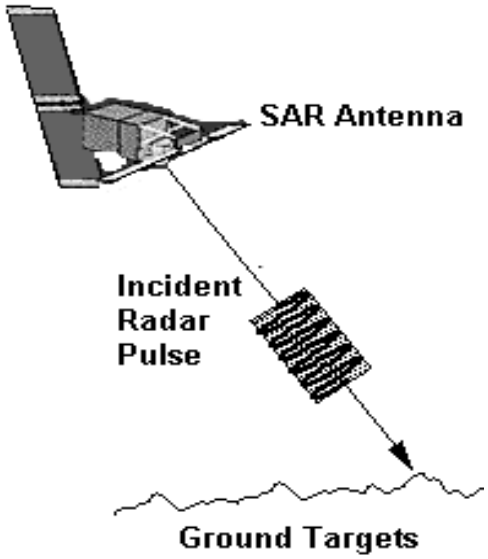

Figure 1.5 Transmitted Radar pulse from SAR antenna to ground

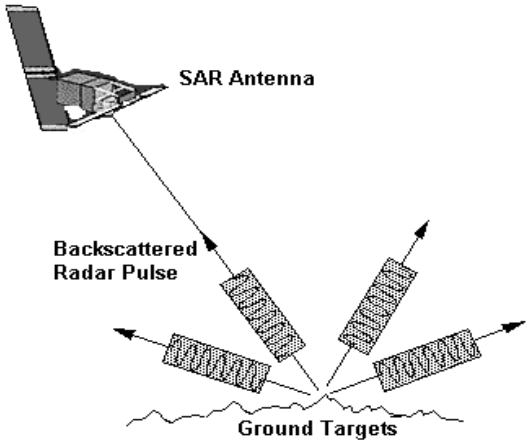

Figure 1.6 Backscattered Radar pulse from ground to SAR antenna

In real aperture radar imaging, the ground resolution is limited by the size of the microwave beam sent out from the antenna. Finer details on the ground can be resolved by using a narrower beam. The beam width is inversely proportional to the size of the antenna, i.e. the longer the antenna, the narrower the beam. The Antenna's Footprint is an area illuminated by the microwave beam sent out by the antenna. In radar imaging, the recorded signal strength depends on the microwave energy backscattered from the ground targets inside this footprint. Increasing the length of the antenna will decrease the width of the footprint. It is not feasible for a spacecraft to carry a very long antenna which is required for high resolution imaging of the earth surface. To overcome this limitation, SAR capitalises on the motion of the space craft to emulate a large antenna from the small antenna it actually carries on board. The following figure shows a SAR image that may be used for testing.

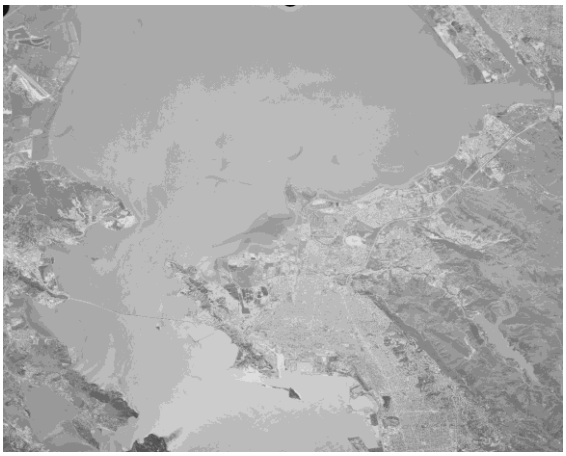

Figure 1.7 A SAR image

Chapter 2

Literature Review

There are many Image Processing methods that have been used to classify SAR images using Texture Analysis till date. Many texture models have been proposed for classification of SAR images like Gray Level Co-occurrence Matrix method, MRF models, Gabor Wavelets etc. A brief literature review is presented below for classification of SAR images using Texture parameters.

In 1973, Haralick et. al. proposed general procedure for extracting textural properties of blocks of image data. These features were calculated in the spatial domain and the statistical nature of texture was taken into account in the procedure, which was based on the assumption that the texture information in an image I was contained in the overall or "average" spatial relationship which the gray tones in the image have to one another. They computed a set of gray tone spatial-dependence probability-distribution matrices for a given image block and suggested a set of 14 textural features, which can be extracted from each of these matrices. These features contained information about such image textural characteristics as homogeneity, gray-tone linear dependencies (linear structure), contrast, number and nature of boundaries present, and the complexity of the image. It was important to note that the number of operations required computing any one of these features was proportional to the number of resolution cells in the image block. It was for this reason that these features were called quickly computable. [2]

In 1988, H.H.Loh et. al. presented a family of texture features that had the ability to discriminate different textures in a 3-D scene as well as the ability to recover the range and orientation of the surfaces of the scene. These texture features were derived from the gray level run length matrices (GLRLM's) of an image. The GLRLM's were first normalized so that they all had equal average gray level run length. Features extracted from the normalized GLRLM's were independent of the surface geometry. Experiments for the discrimination of natural textures had been conducted. The results demonstrated that these features had the ability to discriminate different textures in a nontrivial 3-D scene. [3]

In 1992, Chung-Ming Wu. et.al. studied the classification of ultrasonic liver images by making use of some powerful texture features, including the spatial gray-level

dependence matrices, the Fourier power spectrum, the gray-level difference statistics, and the Laws' texture energy measures. In this paper, features of these types were used to classify three sets of ultrasonic liver images-normal liver, hepatoma, and cirrhosis. [4]

In 1994, D. Patel et. al. performed texture analysis for foreign object detection using a single layer neural network and PCA. The foreign objects (FOs) occur extremely rarely, but their presence causes alarm to both the consumer and the food manufacturer. FOs which can potentially occur in food products varied in form and size; they ranged from hard contaminants such as slivers of glass to soft contaminants such as small pieces of wood. This work presented a method to detect FOs in bags of frozen vegetables and in particular using bags of frozen corn kernels. The final stage of the production process was the inspection process where the bags had been packed and sealed. Then X-ray imaging was used to view the contents of the bag. Convolution masks sensitive to the particular local structural attributes were used to extract texture features and, based on these features, the FOs in the image were detected and segmented. These filters responded to the peculiarities of the structure of the texture and subsequently detected any anomalies, such as FOs within the food substrate. They also used principal component analysis (PCA) techniques to find orthogonal vectors in data space that accounted for as much as possible of the variance of the data. The vectors were then used as the coefficients of the convolution masks. The texture characterisation was based on a convolution operator which "adapts" and "learns" from representation of food samples containing no contaminants using the generalised Hebbian rule. The detected FOs was discrepancies within the food substrate which were highlighted by the convolution process. [5]

In 1995, Anne H. Schistad Solberg et. al. compared the performance of a number of different texture features for SAR image analysis. These features were derived from the gray-level co-occurrence matrix, local statistics, and lognormal random field models. The features were compared based on: (i) their invariance or robustness with respect to natural changes in SAR signatures; and (ii) their discrimination ability and classification accuracy. The invariance of the texture features was investigated on a set of 13 ERS-1 SAR images of the same scene, captured under different conditions. Two main conclusions were drawn from this study, firstly, the texture features were not invariant with respect to natural changes in the mean backscatter values; and secondly,

texture fusion and selection by combining texture features obtained by different models significantly improved the classification accuracy. [6]

In 1995, A.H.Mir et. al. did some work in the use of texture for the extraction of diagnostic information from CT scan images. They obtained a number of features from abdominal CT scans of liver using the spatial domain texture analysis methods. This study investigated that whether texture could be used to discriminate between various tissue types that were inaccessible to human perception and if so, and then what were the most useful parameters. The result was that the texture features were helpful in diagnosing the onset of disease in liver tissue, which cannot be done by visible eye. Three texture features namely - entropy, homogeneity, and gray level distribution were found to be effective. The performance of these features was compared on the basis of significance tests. The results showed that mainly all the parameters could detect the early malignancy with a confidence level of above 99%. [7]

In 2003, Li Ma et. al. in their work described a new scheme for iris recognition from an image sequence. Iris recognition, as an emerging biometric recognition approach, has become a very active topic in both research and practical applications. The main concern of the research was the Iris recognition. First of all, the quality of each image in the input sequence was assessed and a clear iris image was selected. A quality descriptor based on the Fourier spectra of two local regions in an iris image was defined to discriminate clear iris images from low quality images due to motion blur, defocus, and eyelash occlusion. According to the distinct distribution of the iris characteristics, a bank of spatial filters was constructed for efficient feature extraction. A comparative study of existing methods for iris recognition was conducted on an iris image database including 2,255 sequences from 213 subjects. The experimental results demonstrated the effectiveness of the proposed method. A detailed performance comparison of existing methods for iris recognition had been conducted on the CASIA Iris Database. Conclusions based on such a comparison using a nonparametric statistical method (the bootstrap) provided useful information for further research. [8]

In 2006, A.Abhyankar et. al. proposed a novel approach to detect “liveness” associated with fingerprint scanners. The approach was based on underlying texture and density of the fingerprint images. The algorithm combined the features derived from multi resolution texture analysis as well as derived from local ridge frequency

analysis. The features were further processed using FCM and error rates were calculated. Based on the association of all the points to particular type of a class, the classification rates were calculated. The training was performed through PCA and first two components were used to map the data non-linearly. This method was tested for three different types of scanner technologies, namely optical, opto-electrical, capacitive DC. Overall 95.36% classification rate was obtained. Advantages of this method were that it was purely software based and required only one image. [9]

In 2007, N. Agani et. al. proposed an algorithm for texture analysis. The proposed algorithm was a combination of wavelet extension transform with gray level co-occurrence matrix. Texture analysis provides a significant role in identification and classification of surface from medical images and many other types of images. It has a vital role in automatic visual inspection in a number of applications like industrial monitoring of product quality control, remote sensing and medical diagnosis. In this research, medical images of echocardiography (ECG) of heart were used to identify heart with suspected myocardial infarction problem. The wavelet extension transform was used to form image approximation with higher resolution. The gray level co-occurrence matrices were computed for each sub band. These matrices were then used to extract four feature vectors: entropy, contrast, energy (angular second moment) and homogeneity (inverse difference moment). Mahalanobis distance classifier was used in this work. The method was tested with clinical data from echocardiography images of 17 patients. For each patient, tissue samples were taken from suspected infarcted area as well as from non-infarcted (normal) area. For each patient, 8 frames separated by some time interval were used and for each frame, 5 normal regions and 5 suspected myocardial infarction regions of 16×16 pixel size were analyzed. The performance of the proposed method was compared to that energy base of wavelet image extension transform based on energy. It was found that the classification rate obtained using the wavelet extension based on energy technique was 81.62%, while the proposed method achieved 91.32% accuracy. [10]

In 2008, F.Zhang et. al. identified oil spills on the basis of textural information of marine SAR images. Oil spill pollution is a major environmental threat for many countries in the world, which can cause serious damage to marine environment. Synthetic aperture radar (SAR) has become a valuable tool for marine oil spill monitoring, because of its all-weather and all-day capabilities. In this work, co-occurrence matrix method was employed to extract textural features of marine SAR

image first, then these features were analyzed and optimized, and then Support Machine Vector (SVM) method was employed to discriminate oil spill and other look-alikes in SAR images. [11]

In 2009, Vijaya V. Chamundeeswari et. al. analysed the role of various intensity and textural measures for their discriminative ability for unsupervised SAR image classification into various land cover types like water, urban, and vegetation areas. To make the algorithm adaptable, these textural features were fused using principal component analysis (PCA), and principal components were used for classification purposes. To highlight the effectiveness of PCA, the difference between PCA- and non-PCA-based classifications was also analyzed. The analysis of how every individual feature measure contributes for classification process has been presented, and then, textural measures for a feature set were chosen according to their role in improving classification accuracy. By analysis, it was observed that the feature set comprising mean, variance, wavelet components, semivariogram, lacunarity, and weighted rank fill ratio provided good classification accuracy of up to 90.4% than by using individual textural measures, and this increased accuracy justified the complexity involved in the process. [12]

In 2009, Yanning et. al. used texture parameters for assessment of SAR ocean images. They have found some parameters of texture features of two SAR ocean images. Theses parameters were positive modulation, negative modulation, margin of modulations, ratios of modulations etc. They proved that these parameters could evaluate texture feature in certain degree when applied to analyse texture feature in the two SAR ocean images. Compared to traditional parameters applied to land point targets, new parameters could be calculated from images directly, compared to parameters applied to common images which contain texture features, new parameters described the characters of streaks fully, especially the relationship between positive and negative modulation which appeared as the format of bright and dark streaks. At the same time, the process of computing was not difficult so using these parameters to evaluate texture feature was operable. [13]

In 2009, A.Kourgli et. al. developed a new nonparametric MRF model of textures which resulted in a new approach for fast texture analysis, synthesis and classification. The proposed method described a texture by identifying the spatial distribution of its neighbourhoods and deriving a likeness measure of their spatial organization. The identification conducted to the definition of a new nonparametric

MRF model using the likeness measure that provided a consistent estimate of the joint distribution of pixels in a window of optimal size. For texture synthesis, they introduced a multi-scale approach incorporating discrete optimization. As a result, the method lead to fast and efficient texture synthesis and texture identification algorithms. The model proposed seems suitable for the practical application of terrain mapping of SAR images. [14]

A lot of work has been done on use of texture features, frequency spectrum features etc for classification of SAR images. But still there is scope for a simple but effective classification technique based on the above reviewed parameters. The SAR images have been classified using statistical approaches, MRF models and Gabor filters in the review presented above. The proposed simple approach can be used to classify SAR images into land, urban area, water, forest etc which can be useful for numerous applications like map updating, SAR ocean images or classification of a country's SAR image on the basis of forests or urban land.

2.1 PROBLEM FORMULATION

The main motive of our work is to classify SAR images into two categories, water and urban area on the basis of texture features. Texture analysis of these SAR images has been done using statistical approach based on GLCM and GLRLM. The Discriminative power distance is used to find discrimination between different parameters. Then dimension reduction is done using correlation coefficient. Finally, we have proposed a set of texture features for classification of SAR images into water and urban area coverage.

Chapter 3

TEXTURE ANALYSIS

3.1 TEXTURE

Texture is used to describe the feel of non-tactile sensations. Textures are characteristic intensity (or colour) variations that typically originate from roughness of object surfaces. For a well-defined texture, intensity variations will normally exhibit both regularity and randomness and for this reason texture analysis requires careful design of statistical measures.

Texture is a combination of repeated patterns with a regular frequency. In visual interpretation texture has several types, for example, smooth, fine, coarse etc. Texture analysis is defined as the classification or segmentation of textural features with respect to the shape of a small element, density and direction of regularity. Texture provides a way to segment and recognise the surfaces.

There are a number of definitions of texture that have been formulated by different people depending upon the particular application and there are no generally agreed upon definition.

3.2 PROPERTIES OF TEXTURE

- Texture is a property of areas and texture of a point is undefined. So, texture is a contextual property and its definition must involve gray values in a spatial neighbourhood.
- Texture involves the spatial distribution of gray levels. Thus, two-dimensional histograms or co-occurrence matrices are reasonable texture analysis tools.
- Texture in an image can be perceived at different scales or levels of resolution.

3.3 TEXTURE ANALYSIS TYPES

Approaches to texture analysis are usually categorized into:

1. Structural,
2. Statistical,
3. Model-based and
4. Transform

3.3.1 STRUCTURAL APPROACH

Structural approaches represent texture by well defined primitives (micro texture) and a hierarchy of spatial arrangements (macro texture) of those primitives. To describe the texture, one must define the primitives and the placement rules. The choice of a primitive (from a set of primitives) and the probability of the chosen primitive to be placed at a particular location can be a function of location or the primitives near the location. [Haralick, 1979]

The advantage of the structural approach is that it provides a good symbolic description of the image; however, this feature is more useful for synthesis than analysis tasks. The abstract descriptions can be ill defined for natural textures because of the variability of both micro- and macrostructure and no clear distinction between them.

3.3.2 STATISTICAL APPROACH

In contrast to structural methods, statistical approaches do not attempt to understand explicitly the hierarchical structure of the texture. Instead, they represent the texture indirectly by the non-deterministic properties that govern the distributions and relationships between the grey levels of an image. Methods based on second-order statistics (i.e. statistics given by pairs of pixels) have been shown to achieve higher discrimination rates than the power spectrum (transform-based) and structural methods. Accordingly, the textures in grey-level images are discriminated spontaneously only if they differ in second order moments. Equal second order moments, but different third order moments require deliberate cognitive effort.

The statistical approach exploits the statistical properties of image or image regions in a bottom up fashion, starting from the pixel values in the neighbourhood. The co-occurrence matrix is in wide use in representing the dependence in the distributions of gray-level [2]. The co-occurrence matrix is a function of:

1) The image region,

2) A displacement vector $d = (d_x, d_y)$, and

3) The number of gray-levels after quantization.

The matrix contains frequencies of co-occurrence of two gray-levels. After normalization, it becomes a probability matrix with all the elements summing up to 1.

3.3.3 MODEL BASED APPROACH

Model based texture analysis using fractal and stochastic models, attempt to interpret an image texture by use of, respectively, generative image model and stochastic

model. The parameters of the model are estimated and then used for image analysis. In practice, the computational complexity arising in the estimation of stochastic model parameters is the primary problem. The fractal model has been shown to be useful for modelling some natural textures. It can be used also for texture analysis and discrimination; however, it lacks orientation selectivity and is not suitable for describing local image structures.

3.3.4 TRANSFORM BASED APPROACH

Transform methods of texture analysis, such as Fourier and wavelet transforms represent an image in a space whose co-ordinate system has an interpretation that is closely related to the characteristics of a texture (such as frequency or size). Methods based on the Fourier transform perform poorly in practice, due to its lack of spatial localization. Gabor filters provide means for better spatial localization; however, their usefulness is limited in practice because there is usually no single filter resolution at which one can localize a spatial structure in natural textures.

3.4 APPROACH USED - STATISTICAL METHODS

The statistical approach has been used in our work. It is the most widely used and more generally applied method because of its high accuracy and less computation time. Texture statistics is frequently classified into first-order, second-order and high order statistics. They are referring to the gray level distribution of pixel on an image. The gray scale is a black and white image at any given focus of pixel, typically there is a corresponding intensity on a range from 0 (black) to 255(white). That means an image is composed of an array of pixels of varying intensity across the image, the intensity corresponding to the level of greyness from black (0) to white (255) at any particular point in the image.

3.5 GRAY-LEVEL CO-OCCURRENCE MATRICES

The gray-level co-occurrence matrix (GLCM), a frequency matrix, is a useful method for enhancing details and is frequently used as an aid for interpretation of an image. The GLCM is a tabulation of how often different combinations of pixel brightness values (grey levels) occur in an image. The GLCM indicates the frequency of a pair of pixels that are at “exactly the same distance and direction of the displacement vector”.

From this principal, it uses to computes the relationships of pixel intensity to the intensity of its neighbouring pixels which are based on hypothesis that the same gray level configuration is repeated in a texture and pixels that are close together tend to be more related than pixels that are far away from each other. The "graycomatrix" command creates the GLCM by calculating how often a pixel with gray-level (gray scale intensity) value i occurs horizontally adjacent to a pixel with the value j. Each element (i,j) in GLCM specifies the number of times that the pixel with value i occurred horizontally adjacent to a pixel with value j.

The GLCM $P_{(d,\theta)}(l_1,l_2)$ represents the probability of occurrence of the pair of gray levels (l_1,l_2) separated by a given distance d at angle θ. GLCMs are constructed by mapping the gray-level co-occurrence counts or probabilities based on the spatial relations of pixels at different angular directions while scanning the image from left-to-right and top-to-bottom. Typically, four values of θ, namely 0°, 45°, 90° and 135° cover the orientations and most common choice of distance d=1 when θ is 0° or 90° and d= √2 when θ is 45° or 135°.

For an image with number of pixels P=36, gray levels K=4, and pixel values

1	0	2	3	1	2
1	2	3	2	1	1
2	3	2	0	1	2
3	2	1	0	2	2
2	1	1	2	3	2
0	2	2	3	2	1

Let us consider, for example, pairs of pixels positioned diagonally next to each other from left to upper right where d=√2 and θ=45°. A K by K matrix H(d, θ) is formed such that each element h_{ij} is the number of times a pixel with value i and another with value j are located in the selected relative position. For example, the count h_{01} is 3 and the count h_{33} is 4. The complex matrix H (√2, 45°) for this image is

	0	1	2	3
0	0	3	0	0
1	3	2	1	0
2	0	2	9	0
3	0	0	1	4

3.5.1 Order of Texture Measures:

- *First order* texture measures are statistics calculated from the original image values, like variance, and do not consider pixel neighbor relationships.
- *Second order* measures consider the relationship between groups of two (usually neighboring) pixels in the original image.
- *Third and higher order* textures (considering the relationships among three or more pixels) are theoretically possible but not commonly implemented due to calculation time and interpretation difficulty.

Haralick has proposed a number of useful texture features that can be computed from the co-occurrence matrix. Here μ_x and μ_y are the means and σ_x and σ_y are the standard deviations of $P_d(x)$ and $P_d(y)$ respectively.

$$P_d(x) = \Sigma_j P_d(x,j)$$
$$P_d(y) = \Sigma_i P_d(i,y)$$

In order to define Haralick's Texture measures, GLCM is normalised as

$$p(l_1, l_2) = \frac{P(l_1, l_2)}{\sum_{l_1=0}^{L-1} \sum_{l_2=0}^{L-1} P(l_1, l_2)}$$

In the derivation of Haralick's texture measures the following entities are used:

$$p_x(l_1) = \sum_{l_2=0}^{L-1} p(l_1, l_2)$$

$$p_y(l_2) = \sum_{l_1=0}^{L-1} p(l_1, l_2)$$

$$p_{x+y}(k) = \sum_{l_1=0}^{L-1} \sum_{l_2=0}^{L-1} p(l_1, l_2)$$

Where k=0, 1, 2, ... , 2(L-1)

The texture measures are defined as follows:

The **ASM (Angular Second Moment) or Energy** is a measure of homogeneity. A homogeneous image has a small number of entries along the diagonal of the GLCM with large values which leads to large value of ENERGY.

$$f_1 = \sum_{l_1=0}^{L-1} \sum_{l_2=0}^{L-1} p^{\,2}(l_1, l_2)$$

The **contrast feature** is defined as

$$f_2 = \sum_{k=0}^{L-1} k^2 \sum_{l_1=0}^{L-1} \sum_{l_2=0}^{L-1} p\,(l_1, l_2)$$

The **Correlation measure** represents linear dependencies of gray levels, is defined as

$$f_3 = \frac{1}{\sigma_x \sigma_y} \left[\sum_{l_1=0}^{L-1} \sum_{l_2=0}^{L-1} l_1 l_2\; p\,(l_1, l_2) - \mu_x \mu_y \right]$$

Where μ_x and μ_y are the means, and σ_x and σ_y are the standard deviations of p_x and p_y, respectively.

The **sum of squares** feature is given by

$$f_4 = \sum_{l_1=0}^{L-1} \sum_{l_2=0}^{L-1} (l_1 - \mu_f\,)^2\, p\,(l_1, l_2)$$

where μ_f is the mean gray level of the image.

The inverse difference moment (IDM), a measure of local homogeneity, is defined as

$$f_5 = \sum_{l_1=0}^{L-1} \sum_{l_2=0}^{L-1} \frac{1}{1 + (l_1 - l_2)^2} p\,(l_1, l_2)$$

The **Sum Average** feature is given by

$$f_6 = \sum_{k=0}^{2(L-1)} k p_{x+y}(k)$$

The **sum variance** feature is defined as

$$f_7 = \sum_{k=0}^{2(L-1)} (k - f_6)^2 \, p_{x+y}(k)$$

The **sum entropy** feature is defined as

$$f_8 = -\sum_{k=0}^{2(L-1)} p_{x+y}(k) \log_2\left[p_{x+y}(k)\right]$$

Entropy, a measure of non uniformity in the image or the complexity of the texture, is defined as

$$f_9 = -\sum_{l_1=0}^{L-1} \sum_{l_2=0}^{L-1} p(l_1, l_2) \log_2[p(l_1, l_2)]$$

The **difference variance** measure f_{10} is defined as

$$f_{10} = variance\ of\ p_{x-y}$$

The **difference entropy** measure is defined as

$$f_{11} = -\sum_{k=0}^{(L-1)} p_{x-y}(k) \, log_2\left[p_{x-y}(k)\right]$$

Information measures of correlation are

$$f_{12} = \frac{H_{xy} - H_{xy1}}{max\{H_x, H_y\}}$$

And

$$f_{13} = \{1 - exp[-2(H_{xy2} - H_{xy})]\}^2$$

Where $H_{xy} = f_9$; H_x and H_y are the entropies of p_x and p_y, respectively.

3.6 ANOTHER APPROACH: GRAY LEVEL RUN LENGTH MATRIX

A gray level run is a set of consecutive, collinear picture points having the same gray level value. The length of the run is the number of picture points (pixels) in the run. The major reason for the use of the GLRLM's as the bases of the features is that the lengths of the runs reflect the size of the texture elements. For example, if the distance between the surface and the camera is shortened, then the perceived texture elements will be enlarged and the corresponding gray level runs will be lengthened. Hence, the length of the runs is in reverse proportion to the distance between the camera and the object surface. The GLRLM's also contain the information about the alignment of the texture. For a given picture, we can compute a set of the gray level run length matrices (GLRLM's) for runs with any given direction. However, we usually take only four principle directions (0º, 45º, 90º, and 135 º) in computing the run lengths. The matrix element *(i, j)* specifies the number of times that the picture contains a run length ***j*** in the given direction, consisting of points having gray level ***i*** (or lying in gray level range ***i).***

3.6.1 AVERAGE GRAY LEVEL RUN LENGTH (ARL)

In order to make the extracted textural features independent with the surface range and orientation, the GLRLM's need to be normalized. To do so, we need first compute the average gray level run length (ARL) of the GLRLM's. The ARL is one of the most important properties of the GLRLM's used. Let *P (i, j)* be the ***(i,*** j)th entry of a given GLRLM, *M* be the number of gray levels in the image, and *N* be the maximum run length.

The ARL can be computed as

$$ARL = \frac{\sum_{i=1}^{M}\sum_{j=1}^{N} j.P(i,j)}{\sum_{i=1}^{M}\sum_{j=1}^{N} P(i,j)}$$

The denominator in the above equation is the total number of runs in the matrix. In the numerator, each run count is weighted by the length of the run.

3.6.2 RUN LENGTH FEATURES:

Five original features of run-length statistics derived by Galloway are given below. Here, n_r = total number of runs and n_p = number of pixels in the image

Short Run Emphasis (SRE)

$$SRE = \frac{1}{n_r} \sum_{i=1}^{M} \sum_{j=1}^{N} \frac{P(i,j)}{j^2}$$

Long Run Emphasis (LRE)

$$LRE = \frac{1}{n_r} \sum_{i=1}^{M} \sum_{j=1}^{N} P(i,j).j^2$$

Gray Level Non uniformity (GLN)

$$GLN = \frac{1}{n_r} \sum_{i=1}^{M} \left(\sum_{j=1}^{N} P(i,j) \right)^2$$

Run Length Non Uniformity (RLN)

$$RLN = \frac{1}{n_r} \sum_{i=1}^{N} \left(\sum_{j=1}^{M} P(i,j) \right)^2$$

Run Percentage (RP)

$$RP = \frac{n_r}{n_p}$$

Chu et al proposed two new features to extract gray levels information in the GLRLM

Low Gray Level Run Emphasis (LGRE)

$$LGRE = \frac{1}{n_r} \sum_{i=1}^{M} \sum_{j=1}^{N} \frac{P(i,j)}{i^2}$$

High Gray Level Run Emphasis (HGRE)

$$HGRE = \frac{1}{n_r} \sum_{i=1}^{M} \sum_{j=1}^{N} P(i,j).i^2$$

Chapter 4
METHODOLOGY

In the present study, we have attempted to classify SAR images on the basis of WATER and URBAN Area Coverage by studying their textural features.

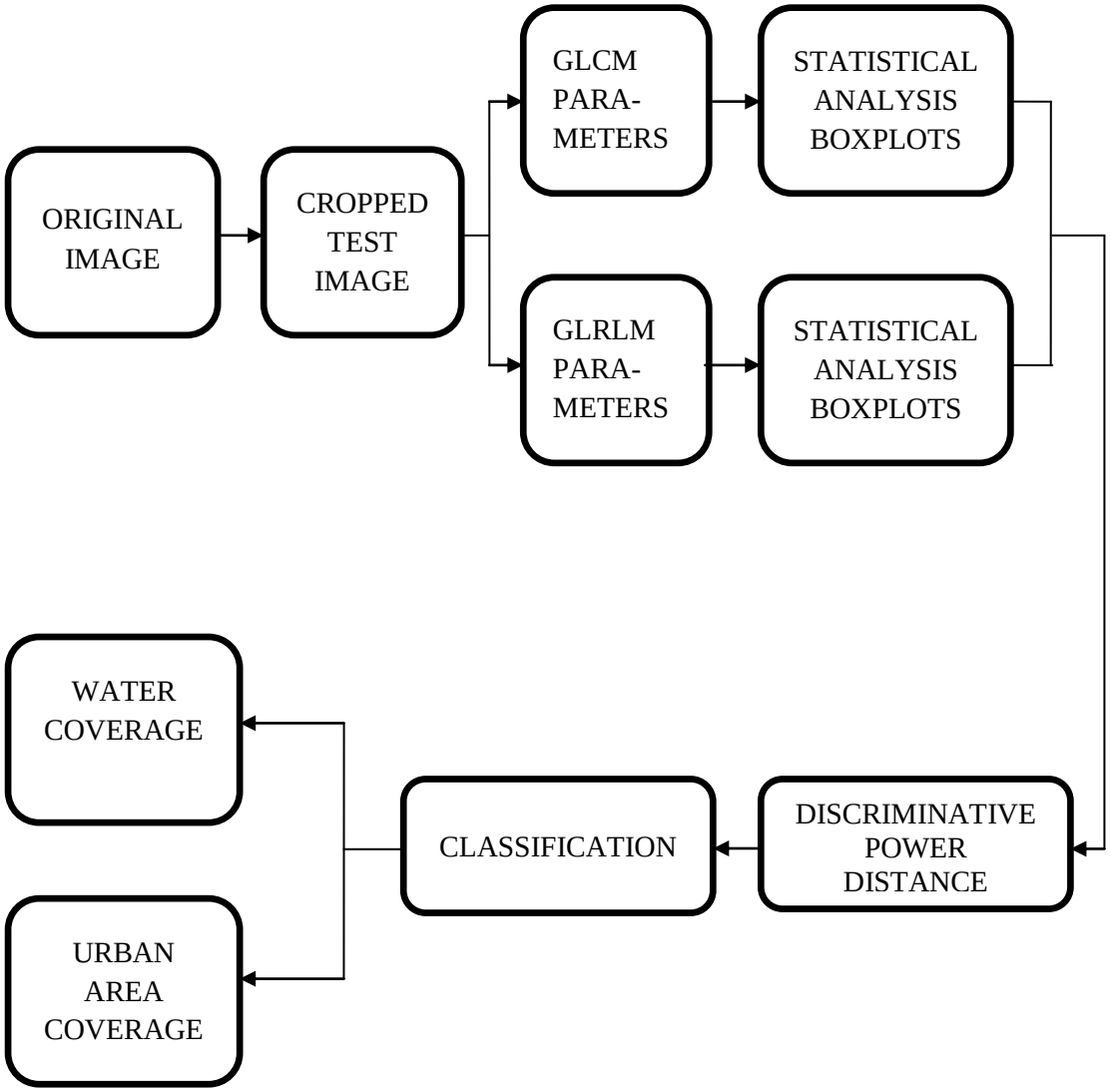

Figure 4.1 Block Diagram for the methodology

Following steps have been performed for the classification:

4.1. IMAGE ACQUISITION

In our work, we have taken the SAR images from database PIEPA (Pilot European Image Processing Archive). The images are analysed to find texture features using GLCM (Gray Level Co occurrence Matrix) and GLRLM (Gray Level Run Length

Matrix) approaches of the texture analysis. By studying their texture features, we have tried to discriminate between them using the statistical nature of the texture features.

4.2. CROPPING THE IMAGE

After acquisition of images, each image is read and is converted from RGB to GRAY. The images that have been used contained both water and urban area coverage. In this study, we needed sub images from different portions of the main image to have urban and water content separately. So, we cropped the image in the window size of 128×128 pixels using the following command:

```
J = imcrop(I,[ xmin ymin 128 128]);
```

In this way, each image is cropped and we have sub images of window size 128×128 pixels.

These sub images are then used to calculate the Gray Level Co-occurrence Matrix (GLCM) and Gray Level Run Length Matrix (GLRLM).

4.3. GRAY LEVEL CO-OCCURENCE MATRIX (GLCM)

The gray level co occurrence matrix of the given images is calculated using MATLAB image processing toolbox. The matrix is calculated for every image and in all the 4 directions that is, 0, 45, 90 and 135.

The following command creates a gray-level co-occurrence matrix (GLCM) from image I.

```
glcm = graycomatrix(I)
```

glcm = graycomatrix(I, param1, val1, param2, val2,...) returns one or more graylevel co-occurrence matrices, depending on the values of the optional parameter/value pairs. Parameter names can be abbreviated, and case does not matter. The various parameters are described in the Table 4.1 below.

Table 4.1. GLCM PARAMETERS

PARAMETER	DESCRIPTION
'GrayLimits'	Two-element vector, [low high], that specifies how the gray scale values in I are linearly scaled into gray levels. Gray scale values less than or equal to low are scaled to 1. Gray scale values greater than or equal to high be scaled to Num Levels. If gray limits is set to [], gray co-matrix uses the minimum and maximum gray scale values in the image as limits, [min (I (:)) max (I (:))].
'NumLevels'	Integer specifying the number of gray-levels to use when scaling the gray scale values in I. For example, if Num Levels is 8, gray co-matrix scales the values in I so they are integers between 1 and 8. The number of gray-levels determines the size of the gray-level co-occurrence matrix (GLCM).
'Offset'	P-by-2 array of integers specifying the distance between the pixel of interest and its neighbour. Each row in the array is a two-element vector, [row_offset, col_offset], that specifies the relationship, or offset, of a pair of pixels. row_offset is the number of rows between the pixel-of-interest and its neighbor. col_offset is the number of columns between the pixel-of-interest and its neighbor. Because the offset is often expressed as an angle, the following table lists the offset values that specify common angles, given the pixel distance D. Angle Offset 0 [0 D] 45 [-D D] 90 [-D 0] 135 [-D -D] D is 1 in our study.
'Symmetric'	A Boolean that creates a GLCM where the ordering of values in the pixel pairs is not considered. For example, when calculating the number of times the value 1 is adjacent to the value 2, gray co-matrix counts both (1,2) and (2,1) pairings, if 'Symmetric' is set to true. When 'Symmetric' is set to false, gray co-matrix only counts 1,2 or 2,1, depending on the value of 'offset'. The GLCM created when 'Symmetric' is set to true is symmetric across its diagonal, and is equivalent to the GLCM described by Haralick (1973).

GLCM of images is calculated using the following syntax:

```
GLCM = graycomatrix(I,'Offset',[0 1]);
```

The offset value is used to determine the distance and direction of pixel neighbour. [0 1] is the default value, that is, 0° direction in which the relation between the gray level value of pixel of interest is found out relative to its next right neighbour. We have used four different directions to calculate the values of GLCM, that is, 0°, 45°, 90° and 135°.

4.4. Properties of GLCM

After GLCM of images are calculated, the textural features of images are calculated using the following command and some programs.

stats = graycoprops(GLCM, properties)

The above command calculates the statistics specified in properties from the gray-level co-occurrence matrix (GLCM). The 'graycoprops' command normalizes the gray-level co-occurrence matrix (GLCM) so that the sum of its elements is equal to 1. Each element (r,c) in the normalized GLCM is the joint probability occurrence of pixel pairs with a defined spatial relationship having gray level values r and c in the image. The 'graycoprops' command uses the normalized GLCM to calculate properties. The properties can be a comma-separated list of strings, a cell array containing strings, the string 'all', or a space separated string. The property names can be abbreviated and are not case sensitive.

Haralick has proposed a number of useful texture features that can be computed from the co-occurrence matrix. Following are the texture features which are found for each image using GLCM and some program codes:

- ASM (Angular Second Moment) or Energy
- Contrast
- Correlation
- Variance
- Inverse difference moment (IDM)
- Entropy
- Sum Average
- Sum Variance
- Sum Entropy
- Difference Variance
- Difference Entropy

- Information measures of Correlation

After finding these features in all the four directions, mean of all the directions is taken. Each figure has given a matrix of 1×13, which is transposed to get a matrix of 13×1. In this way, we have calculated the features for all the images and formed a training set of our data. The results obtained (that will be shown in next chapter) are then used to test a given set of images. Finally, we are able to classify the images.

4.5. GRAY LEVEL RUN LENGTH MATRIX (GLRLM)

GLRLM computes the gray-level run length (GLRL) matrix used for textural analysis of an image using zigzag scan method. The method includes four basic steps

Step 1. Determine direction

Step 2. Zigzag scan

Step 3. Obtain new sequences

Step 4. Calculate run-length matrix

GLRLMS = GRAYRLMATRIX (I, PARAM1, VALUE1, PARAM2, VALUE2 ...) returns one or more gray-level run-length matrices, depending on the values of the optional parameter/value pairs. Parameter names can be abbreviated, and case does not matter. Table 4.2 below describes the GLRLM parameters

TABLE 4.2. GLRLM PARAMETERS

PARAMETER	DESCRIPTION
'GrayLimits'	Two-element vector, [low high], that specifies how the gray scale values in I are linearly scaled into gray levels. Gray scale values less than or equal to low are scaled to 1. Gray scale values greater than or equal to high be scaled to high. If gray limits is set to [], grayrlmatrix uses the minimum and maximum gray scale values in the image as limits, [min(I(:))max(I(:))].
'NumLevels'	Integer specifying the number of gray-levels to use when scaling the grayscale values in I. For example, if NumLevels is 8, GRAYRLMATRIX scales the values in I so they are integers between 1 and 8. The number of gray-levels determines the size of the gray-level run length matrix. 'NumLevels' must be an integer. 'NumLevels' must be 2 if I is logical.
'Offset'	A p-by-1 vector of offsets specifying the scanning direction. Angle Offset 0 1 45 2 90 3 135 4

.

4.6. Properties of GLRLM

After GLRLM of images is calculated, the textural features of images are calculated using the following command and some programs.

stats = graycoprops(GLRLM, properties)

The above command calculates the statistics specified in properties from the gray-level run length matrix GLRLM. Each element in GLRLM (r,c), is the probability occurrence of pixel having gray level values r, run-length c in the image. The properties can be a comma-separated list of strings, a cell array containing strings, the string 'all', or a space separated string. The property names can be abbreviated and are not case sensitive.

Galloway has proposed a number of useful texture features that can be computed from the run length matrix.

Following are the texture features which were found for each image using GLRLM and some program codes:

- SRE
- LRE
- GLN
- RLN
- RP
- LGRE
- HGRE

Chapter 5

RESULTS AND DISCUSSION

5.1. INTRODUCTION

All the 20 texture parameters of the SAR images have been found on the basis of GLCM and GLRLM. The training set for the sub images of water as well as urban area coverage have been formed. On the basis of this training set 13 texture parameters on the basis of GLCM have been found in all the four directions. Along with, 7 GLRLM parameters have also been found. The whole procedure is described below step by step:

- 30 sub images each of water and urban area are used to form two separate training sets.
- GLCM is used to find 13 texture parameters in all the four directions.
- The mean of all the four directions' values is taken.
- GLRLM is used to find 7 texture parameters.
- BOXPLOTS of the training data for water and urban area coverage are then plotted. On the basis of box plots, we can find out which texture measure being computed is of our concern as will be shown later in this section.

5.2 TEST IMAGES

Test images contain Training and Evaluation images. These images are taken from Image database of Essex University (UK). Some of the test images are shown in the next pages.

Figure 5.1 IMAGE 003

Figure 5.2 IMAGE 004

The above shown images are some of the images which are used to make the training set of water sub images. The cropped sub images are shown.

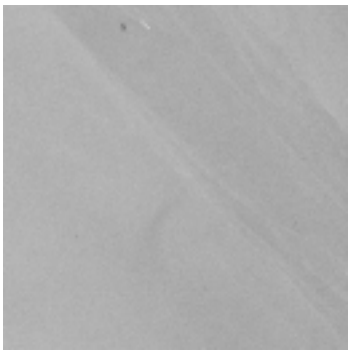

Figure 5.3 IMAGE 003a

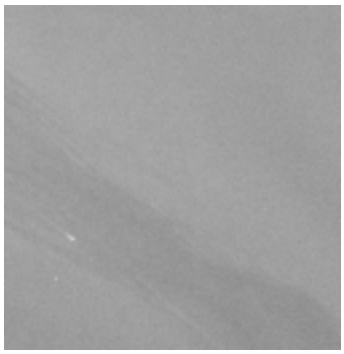

Figure 5.4 IMAGE 003b

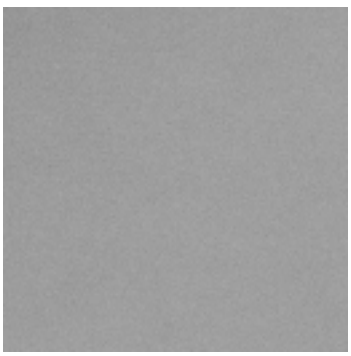

Figure 5.5 IMAGE 004a

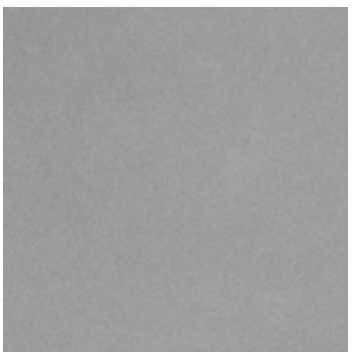

Figure 5.6 IMAGE 004b

The images that are used to make the training set for Urban Area Coverage are as shown:

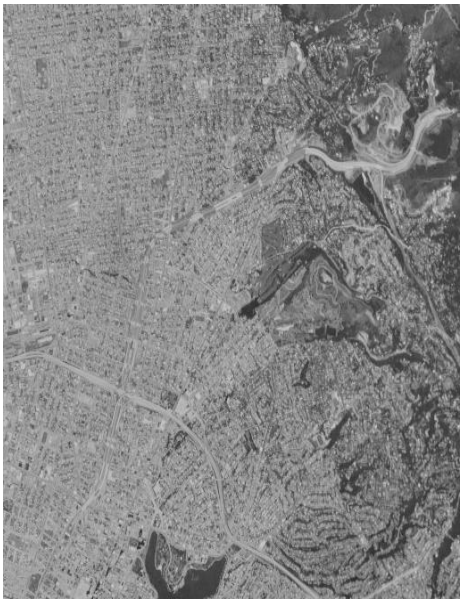

Figure 5.7 IMAGE 014

Figure 5.8 IMAGE 015

The above shown images are some of the images used to make the training set of urban area coverage sub images. Some of the cropped sub images are shown below.

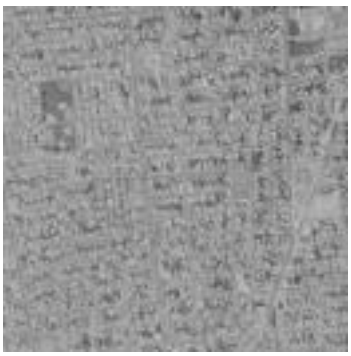

Figure 5.9 IMAGE 014a

Figure 5.10 IMAGE 014b

In this way, we are able to form two training sets:

- Water Training set containing 30 sub images
- Urban Area Training Set containing 30 sub images

5.3. OBSERVATIONS:

Using GLCM, we have calculated 13 texture features in all the four directions, that is, 0°, 45°, 90° and 135°. These are shown in tabular form in the next pages. The last column of each table contains mean of all the four directions. Each table has 30 number of sub images. The images are numbered from 1 to 30. Similarly, 7 features of GLRLM are also tabulated. The two training sets are shown separately.

5.3.1 GLCM FEATURES OF WATER COVERAGE

Table 5.1 ASM VALUES OF WATER

ANGLE-> IMAGE NUMBER	0°	45°	90°	135°	MEAN
1	0.9645	0.9662	0.9652	0.9613	0.9643
2	0.7311	0.7298	0.733	0.7319	0.7314
3	0.9935	0.9933	0.9938	0.9934	0.9935
4	0.9191	0.9193	0.9208	0.9187	0.9195
5	0.9821	0.982	0.9813	0.9819	0.9818
6	0.5633	0.5526	0.56	0.562	0.5595
7	0.9921	0.992	0.992	0.9921	0.992
8	0.9112	0.9104	0.9102	0.9108	0.9106
9	0.94	0.9401	0.9399	0.9397	0.9399
10	0.9842	0.983	0.983	0.9835	0.9834
11	0.6301	0.6196	0.6206	0.6187	0.6222
12	0.7984	0.7935	0.7977	0.7944	0.796
13	0.8664	0.8621	0.8648	0.8638	0.8643
14	0.3421	0.3365	0.348	0.3418	0.3421
15	0.6107	0.6081	0.6116	0.6108	0.6103
16	0.9188	0.918	0.9215	0.92	0.9196
17	0.8982	0.8979	0.8958	0.8976	0.8974
18	0.9399	0.9387	0.9407	0.941	0.9401
19	0.9869	0.9851	0.986	0.9869	0.9862
20	0.9673	0.9671	0.9686	0.9671	0.9675
21	0.8823	0.8804	0.8812	0.8836	0.8819
22	0.9108	0.9117	0.9126	0.9103	0.9114
23	0.9921	0.992	0.9938	0.992	0.9925
24	0.9908	0.9899	0.9905	0.9908	0.9905
25	0.9786	0.9776	0.9778	0.9776	0.9779
26	0.9931	0.9928	0.9932	0.9931	0.9931

27	0.7506	0.7288	0.7266	0.7282	0.7335
28	0.986	0.9871	0.9871	0.987	0.9868
29	0.9849	0.9853	0.9854	0.9855	0.9853
30	0.7694	0.7579	0.7672	0.765	0.7649

Table 5.2 CONTRAST VALUES OF WATER

ANGLE-> IMAGE NUMBER	0°	45°	90°	135°	MEAN
1	0.0158	0.0139	0.016	0.0221	0.017
2	0.065	0.0657	0.0622	0.0634	0.0641
3	0.0041	0.0044	0.0029	0.0044	0.004
4	0.0388	0.0402	0.0368	0.0408	0.0392
5	0.0085	0.0086	0.0086	0.0087	0.0086
6	0.1435	0.1575	0.1472	0.1438	0.148
7	0.0039	0.0041	0.0031	0.004	0.0038
8	0.0446	0.0457	0.0458	0.0453	0.0454
9	0.0294	0.0292	0.0296	0.0295	0.0294
10	0.0071	0.0083	0.0079	0.0078	0.0078
11	0.1561	0.1717	0.1679	0.173	0.1672
12	0.0841	0.0899	0.0859	0.0888	0.0872
13	0.0647	0.0697	0.0669	0.0677	0.0673
14	0.1965	0.2059	0.187	0.1971	0.1966
15	0.1368	0.1412	0.1337	0.1376	0.1373
16	0.0337	0.0346	0.0308	0.0324	0.0329
17	0.0474	0.0479	0.0493	0.0482	0.0482
18	0.0178	0.0191	0.0164	0.0167	0.0175
19	0.0036	0.0054	0.0045	0.0035	0.0043
20	0.0143	0.0148	0.0134	0.0148	0.0143
21	0.0414	0.0436	0.0417	0.0402	0.0417
22	0.9108	0.9117	0.9126	0.9103	0.0354
23	0.0038	0.004	0.0021	0.004	0.0035
24	0.004	0.0049	0.0044	0.004	0.0043
25	0.0104	0.0119	0.0116	0.0119	0.0114
26	0.0033	0.0036	0.0032	0.0034	0.0034
27	0.0949	0.1249	0.1283	0.1256	0.1184
28	0.0063	0.0059	0.0059	0.006	0.006
29	0.0069	0.0069	0.0068	0.0067	0.0068
30	0.0836	0.0963	0.0833	0.0875	0.0877

Table 5.3 CORRELATION VALUES OF WATER

ANGLE-> IMAGE NUMBER	0°	45°	90°	135°	MEAN
1	0.4335	0.5019	0.4223	0.2091	0.3917
2	0.6877	0.6855	0.702	0.6966	0.693
3	0.4129	0.3784	0.5856	0.3784	0.4388
4	0.2544	0.2229	0.2885	0.2112	0.2442
5	0.1523	0.142	0.1894	0.13	0.1534
6	0.5432	0.5003	0.5324	0.5438	0.5299
7	0.1351	0.108	0.409	0.1351	0.1968
8	0.0335	0.0077	0.0048	0.0157	0.0154
9	0.0646	0.0764	0.0607	0.0648	0.0666
10	0.1898	0.0515	0.1285	0.1073	0.1193
11	0.3447	0.2793	0.2996	0.2737	0.2993
12	0.3244	0.2789	0.3065	0.2877	0.2994
13	0.1141	0.0467	0.0814	0.075	0.0793
14	0.6069	0.5881	0.6261	0.6057	0.6067
15	0.4957	0.4782	0.5095	0.4913	0.4937
16	0.3059	0.2883	0.3677	0.3334	0.3238
17	0.1645	0.1536	0.1406	0.1471	0.1514
18	0.5827	0.5513	0.6199	0.6089	0.5907
19	0.6184	0.4403	0.5294	0.6311	0.5548
20	0.2315	0.1906	0.2639	0.1906	0.2192
21	0.47	0.4407	0.4705	0.4844	0.4664
22	0.3454	0.3532	0.3739	0.3239	0.3491
23	0.0579	0.028	0.4991	0.028	0.1532
24	0.2306	0.0673	0.1606	0.2305	0.1723
25	0.1352	0.0146	0.0537	0.0146	0.0545
26	0.0984	-0.0018	0.1001	0.0661	0.0657
27	0.4197	0.2283	0.2063	0.2245	0.2697
28	0.1844	0.154	0.1688	0.137	0.1611
29	0.1583	0.1208	0.1208	0.1519	0.1379
30	0.46	0.3821	0.4694	0.4385	0.4375

Table 5.4 DIFFERENCE ENTROPY VALUES OF WATER

ANGLE-> IMAGE NUMBER	0°	45°	90°	135°	MEAN
1	0.0347	0.031	0.034	0.0414	0.0353
2	0.1045	0.1053	0.1012	0.1025	0.1034
3	0.0094	0.0097	0.0079	0.0097	0.0092
4	0.0708	0.0717	0.068	0.0727	0.0708
5	0.0211	0.0213	0.0215	0.0215	0.0214
6	0.1786	0.1892	0.1815	0.1789	0.182
7	0.0109	0.0112	0.0092	0.0109	0.0106
8	0.0792	0.0806	0.0808	0.0801	0.0802
9	0.0577	0.0573	0.0578	0.0578	0.0576
10	0.0183	0.0209	0.0201	0.0198	0.0198
11	0.1881	0.1991	0.1965	0.2001	0.196
12	0.1254	0.1313	0.1272	0.1302	0.1285
13	0.1042	0.1098	0.1067	0.1075	0.107
14	0.2152	0.2208	0.2092	0.2156	0.2152
15	0.1733	0.1768	0.1709	0.174	0.1738
16	0.0641	0.0653	0.0597	0.0621	0.0628
17	0.0828	0.0834	0.0853	0.0839	0.0839
18	0.0388	0.0411	0.0364	0.0368	0.0383
19	0.0104	0.0145	0.0125	0.0102	0.0119
20	0.0325	0.0335	0.0308	0.0335	0.0326
21	0.0748	0.0778	0.0753	0.0732	0.0753
22	0.067	0.0661	0.0646	0.0684	0.0665
23	0.0109	0.0112	0.0064	0.0112	0.01
24	0.0113	0.0134	0.0122	0.0114	0.0121
25	0.025	0.0271	0.0265	0.0271	0.0264
26	0.0095	0.0104	0.0094	0.0098	0.0098
27	0.1363	0.1636	0.1664	0.1641	0.1576
28	0.0166	0.0158	0.0156	0.016	0.016
29	0.0179	0.0179	0.0178	0.0174	0.0177
30	0.1248	0.1377	0.1246	0.1289	0.129

Table 5.5 DIFFERENCE VARIANCE VALUES OF WATER

ANGLE-> IMAGE NUMBER	0°	45°	90°	135°	MEAN
1	0.0159	0.014	0.0162	0.0222	0.0171
2	0.0623	0.0629	0.0598	0.0609	0.0615
3	0.0041	0.0044	0.0029	0.0044	0.004
4	0.0384	0.0398	0.0365	0.0403	0.0388
5	0.0086	0.0087	0.0087	0.0088	0.0087
6	0.1241	0.1337	0.1267	0.1244	0.1272
7	0.004	0.0041	0.0032	0.004	0.0038
8	0.0438	0.0448	0.045	0.0444	0.0445
9	0.0294	0.0291	0.0295	0.0295	0.0294
10	0.0072	0.0084	0.008	0.0079	0.0079
11	0.1327	0.143	0.1405	0.1438	0.14
12	0.0787	0.0835	0.0802	0.0826	0.0812
13	0.0621	0.0665	0.064	0.0647	0.0643
14	0.1583	0.1637	0.1525	0.1586	0.1583
15	0.1194	0.1226	0.1172	0.12	0.1198
16	0.0335	0.0344	0.0307	0.0322	0.0327
17	0.0464	0.0468	0.0482	0.0472	0.0471
18	0.0179	0.0192	0.0165	0.0168	0.0176
19	0.0037	0.0054	0.0045	0.0036	0.0043
20	0.0144	0.015	0.0135	0.015	0.0145
21	0.0408	0.0429	0.0411	0.0396	0.0411
22	0.0355	0.0349	0.0339	0.0364	0.0352
23	0.0039	0.004	0.0021	0.004	0.0035
24	0.004	0.0049	0.0044	0.0041	0.0044
25	0.0105	0.012	0.0117	0.012	0.0116
26	0.0033	0.0036	0.0032	0.0034	0.0034
27	0.0876	0.1108	0.1133	0.1113	0.1058
28	0.0064	0.006	0.0059	0.0061	0.0061
29	0.007	0.007	0.0069	0.0067	0.0069
30	0.0784	0.0888	0.0781	0.0816	0.0817

Table 5.6 ENTROPY VALUES OF WATER

ANGLE-> IMAGE NUMBER	0°	45°	90°	135°	MEAN
1	0.0499	0.0484	0.0498	0.0534	0.0504
2	0.2485	0.2496	0.2463	0.2475	0.248
3	0.0119	0.012	0.0112	0.012	0.0118
4	0.0956	0.0959	0.0943	0.0961	0.0955
5	0.0266	0.0266	0.0276	0.0266	0.0268
6	0.3754	0.3843	0.3781	0.3762	0.3785
7	0.0137	0.0139	0.0143	0.0138	0.0139
8	0.097	0.0969	0.097	0.0969	0.097
9	0.0707	0.0708	0.0708	0.071	0.0708
10	0.0234	0.0243	0.0247	0.024	0.0241
11	0.3292	0.3356	0.3354	0.3361	0.3341
12	0.2	0.2031	0.2003	0.2026	0.2015
13	0.1396	0.1411	0.14	0.1406	0.1403
14	0.5162	0.5219	0.5102	0.5166	0.5162
15	0.343	0.3451	0.342	0.343	0.3433
16	0.0944	0.0951	0.0923	0.0935	0.0938
17	0.1118	0.1118	0.1135	0.112	0.1123
18	0.074	0.0753	0.0729	0.0726	0.0737
19	0.0203	0.0228	0.0215	0.0203	0.0212
20	0.0437	0.0438	0.0424	0.0438	0.0434
21	0.1294	0.1311	0.1304	0.1283	0.1298
22	0.1024	0.1016	0.1009	0.1028	0.1019
23	0.0127	0.0128	0.0108	0.0128	0.0123
24	0.0147	0.0156	0.0151	0.0148	0.0151
25	0.0302	0.031	0.0312	0.031	0.0309
26	0.0113	0.0114	0.0111	0.0113	0.0113
27	0.2391	0.2526	0.2535	0.2528	0.2495
28	0.0211	0.0196	0.0196	0.0196	0.02
29	0.0224	0.0218	0.0216	0.0216	0.0219
30	0.2252	0.234	0.2267	0.2286	0.2286

Table 5.7 INVERSE DIFFERENCE MOMENT (IDM) VALUES OF WATER

ANGLE-> IMAGE NUMBER	0°	45°	90°	135°	MEAN
1	0.9923	0.9934	0.9926	0.9907	0.9922
2	0.9675	0.9672	0.9689	0.9683	0.968
3	0.9984	0.9984	0.9987	0.9984	0.9985
4	0.9809	0.9809	0.982	0.9805	0.9811
5	0.9958	0.9958	0.9957	0.9957	0.9958
6	0.9282	0.9213	0.9264	0.9281	0.926
7	0.9981	0.998	0.9984	0.9981	0.9982
8	0.9777	0.9772	0.9771	0.9774	0.9774
9	0.9853	0.9854	0.9852	0.9852	0.9853
10	0.9965	0.9958	0.996	0.9961	0.9961
11	0.922	0.9142	0.9161	0.9135	0.9164
12	0.9579	0.955	0.9571	0.9556	0.9564
13	0.9676	0.9651	0.9665	0.9662	0.9664
14	0.9017	0.897	0.9065	0.9014	0.9017
15	0.9316	0.9294	0.9331	0.9312	0.9313
16	0.9831	0.9827	0.9846	0.9838	0.9836
17	0.9763	0.9761	0.9754	0.9759	0.9759
18	0.9911	0.9904	0.9918	0.9917	0.9913
19	0.9982	0.9973	0.9978	0.9982	0.9979
20	0.9929	0.9926	0.9933	0.9926	0.9928
21	0.9793	0.9782	0.9791	0.9799	0.9791
22	0.9821	0.9824	0.983	0.9816	0.9823
23	0.9981	0.998	0.999	0.998	0.9983
24	0.998	0.9976	0.9978	0.998	0.9978
25	0.9949	0.9944	0.9945	0.9944	0.9945
26	0.9984	0.9982	0.9984	0.9983	0.9983
27	0.9525	0.9375	0.9359	0.9372	0.9408
28	0.9969	0.997	0.9971	0.997	0.997
29	0.9965	0.9966	0.9966	0.9967	0.9966
30	0.9584	0.952	0.9584	0.9564	0.9563

Table 5.8 INFORMATION MEASURE OF CORRELATION 1 VALUES OF WATER

ANGLE-> IMAGE NUMBER	0°	45°	90°	135°	MEAN
1	-2.7963	-2.8441	-2.7937	-2.676	-2.7775
2	-3.0164	-3.0081	-3.0418	-3.0326	-3.0247
3	-2.7905	-2.7736	-2.885	-2.7786	-2.8069
4	-2.6713	-2.6705	-2.6833	-2.6246	-2.6624
5	-2.5345	-2.5501	-2.6626	-2.5072	-2.5636
6	-2.8474	-2.8157	-2.8396	-2.8427	-2.8364
7	-2.4161	-2.402	-2.8944	-2.4178	-2.5326
8	-2.5907	-2.6001	-2.5821	-2.5651	-2.5845
9	-2.6106	-2.6068	-2.6093	-2.6186	-2.6113
10	-2.5932	-2.5065	-2.643	-2.5588	-2.5754
11	-2.7158	-2.6743	-2.683	-2.6679	-2.6852
12	-2.7252	-2.6975	-2.7132	-2.7009	-2.7092
13	-2.6297	-2.5978	-2.6067	-2.6048	-2.6098
14	-2.8902	-2.8715	-2.9101	-2.8889	-2.8902
15	-2.801	-2.7754	-2.82	-2.8095	-2.8015
16	-2.7225	-2.6955	-2.7696	-2.7573	-2.7362
17	-2.613	-2.5957	-2.6305	-2.6167	-2.614
18	-2.9314	-2.9215	-2.9981	-2.9366	-2.9469
19	-3.0629	-2.8886	-2.972	-3.0764	-3
20	-2.7113	-2.6363	-2.6835	-2.6363	-2.6669
21	-2.8108	-2.767	-2.8324	-2.8429	-2.8133
22	-2.7448	-2.7215	-2.7569	-2.7408	-2.741
23	-2.8129	-2.8004	-2.9598	-2.8004	-2.8434
24	-2.7307	-2.6291	-2.6829	-2.7306	-2.6933
25	-2.6081	-2.5736	-2.6097	-2.552	-2.5859
26	-2.6479	-2.5682	-2.6112	-2.5928	-2.605
27	-2.7745	-2.6394	-2.6222	-2.6232	-2.6648
28	-2.6589	-2.5166	-2.4974	-2.4476	-2.5301
29	-2.6764	-2.542	-2.5421	-2.5595	-2.58
30	-2.7954	-2.7362	-2.8254	-2.778	-2.7838

Table 5.9 INFORMATION MEASURE OF CORRELATION 2 VALUES OF WATER

ANGLE-> IMAGE NUMBER	0°	45°	90°	135°	MEAN
1	0.3792	0.3826	0.3783	0.3712	0.3778
2	0.7846	0.785	0.7865	0.7861	0.7856
3	0.1892	0.1893	0.1923	0.1894	0.19
4	0.4857	0.4832	0.4863	0.4828	0.4845
5	0.2662	0.2655	0.273	0.2655	0.2676
6	0.8403	0.838	0.8399	0.8409	0.8398
7	0.1927	0.1927	0.2176	0.1934	0.1991
8	0.4733	0.4724	0.4726	0.4724	0.4727
9	0.4125	0.4133	0.4124	0.4131	0.4128
10	0.2528	0.2494	0.2553	0.2507	0.252
11	0.7826	0.7795	0.7815	0.7793	0.7807
12	0.6635	0.6612	0.6615	0.6617	0.662
13	0.5574	0.5557	0.5559	0.5566	0.5564
14	0.908	0.9069	0.9092	0.9079	0.908
15	0.8136	0.812	0.8153	0.8129	0.8134
16	0.4923	0.4915	0.496	0.4939	0.4934
17	0.5121	0.5112	0.5133	0.511	0.5119
18	0.4879	0.4853	0.4927	0.4895	0.4889
19	0.2784	0.2716	0.2744	0.2799	0.2761
20	0.3431	0.3395	0.3413	0.3395	0.3409
21	0.5864	0.584	0.5882	0.5871	0.5864
22	0.5148	0.5142	0.5157	0.5125	0.5143
23	0.1818	0.182	0.1949	0.182	0.1852
24	0.205	0.2019	0.2032	0.2056	0.2039
25	0.281	0.2789	0.2811	0.2789	0.28
26	0.1734	0.1714	0.1722	0.1722	0.1723
27	0.7199	0.7075	0.7062	0.7074	0.7102
28	0.2402	0.2297	0.231	0.2292	0.2325
29	0.2454	0.24	0.2392	0.2408	0.2414
30	0.7129	0.709	0.7164	0.7127	0.7127

Table 5.10 SUM AVERAGE VALUES OF WATER

ANGLE-> IMAGE NUMBER	0°	45°	90°	135°	MEAN
1	8.0228	8.0228	8.0227	8.0228	8.0228
2	10.2357	10.2366	10.2364	10.2366	10.2363
3	10.0046	10.0046	10.0046	10.0046	10.0046
4	10.0488	10.0485	10.0486	10.0485	10.0486
5	11.9906	11.9907	11.9901	11.9907	11.9905
6	10.39	10.3916	10.391	10.3917	10.3911
7	11.998	11.998	11.9988	11.998	11.9982
8	10.0473	10.0471	10.0472	10.0471	10.0472
9	10.032	10.0321	10.032	10.0321	10.032
10	11.9912	11.9912	11.9909	11.9912	11.9911
11	11.7237	11.7236	11.7215	11.7236	11.7231
12	11.8666	11.8664	11.8674	11.8664	11.8667
13	11.9251	11.925	11.9253	11.925	11.9251
14	10.9913	10.9915	10.9922	10.9913	10.9916
15	11.6764	11.6774	11.6744	11.6774	11.6764
16	11.9502	11.9501	11.9501	11.9501	11.9501
17	11.9416	11.9418	11.9409	11.9418	11.9415
18	11.9564	11.9565	11.9559	11.9565	11.9563
19	11.9904	11.9904	11.9904	11.9904	11.9904
20	10.0188	10.0185	10.0184	10.0185	10.0185
21	10.0813	10.0812	10.0822	10.0812	10.0815
22	10.0563	10.0559	10.056	10.0559	10.056
23	10.0039	10.004	10.0039	10.004	10.0039
24	10.0052	10.0052	10.0052	10.0052	10.0052
25	9.9884	9.9883	9.9882	9.9883	9.9883
26	9.9964	9.9964	9.9964	9.9964	9.9964
27	10.1797	10.1777	10.1773	10.1777	10.1781
28	10.0078	10.007	10.0071	10.007	10.0072
29	10.0082	10.0079	10.0078	10.0079	10.0079
30	12.1679	12.1692	12.1707	12.1692	12.1692

Table 5.11 SUM ENTROPY VALUES OF WATER

ANGLE-> IMAGE NUMBER	0°	45°	90°	135°	MEAN
1	0.0451	0.0441	0.0448	0.0472	0.0453
2	0.229	0.2299	0.2276	0.2284	0.2287
3	0.011	0.0112	0.0104	0.0111	0.0109
4	0.0838	0.0836	0.0831	0.0837	0.0836
5	0.0241	0.024	0.025	0.024	0.0243
6	0.3322	0.3367	0.3337	0.3329	0.3339
7	0.0127	0.0129	0.0134	0.0128	0.013
8	0.0836	0.0832	0.0832	0.0832	0.0833
9	0.0619	0.062	0.0619	0.0621	0.062
10	0.0213	0.0218	0.0223	0.0217	0.0218
11	0.2822	0.284	0.2848	0.284	0.2838
12	0.1746	0.1761	0.1744	0.1758	0.1752
13	0.1201	0.1201	0.1198	0.1202	0.1201
14	0.4571	0.4599	0.454	0.4573	0.457
15	0.3018	0.3026	0.3018	0.3016	0.302
16	0.0843	0.0847	0.083	0.0837	0.0839
17	0.0975	0.0974	0.0987	0.0975	0.0978
18	0.0687	0.0696	0.068	0.0676	0.0685
19	0.0192	0.0211	0.0202	0.0192	0.0199
20	0.0394	0.0393	0.0384	0.0393	0.0391
21	0.117	0.118	0.1179	0.1162	0.1173
22	0.0917	0.091	0.0906	0.0917	0.0913
23	0.0115	0.0117	0.0101	0.0117	0.0113
24	0.0135	0.0142	0.0138	0.0136	0.0138
25	0.0271	0.0276	0.0277	0.0276	0.0275
26	0.0103	0.0104	0.0102	0.0103	0.0103
27	0.2106	0.215	0.2149	0.2151	0.2139
28	0.0192	0.0178	0.0179	0.0179	0.0182
29	0.0203	0.0197	0.0196	0.0196	0.0198
30	0.2001	0.2051	0.2017	0.2024	0.2023

Table 5.12 SUM VARIANCE VALUES OF WATER

ANGLE-> IMAGE NUMBER	0°	45°	90°	135°	MEAN
1	63.6846	63.7017	63.6862	63.6451	63.6794
2	100.4846	100.4861	100.5315	100.5176	100.505
3	99.8827	99.8789	99.8953	99.881	99.8845
4	99.3669	99.3617	99.3775	99.3594	99.3664
5	143.2095	143.2114	143.175	143.2126	143.2021
6	101.6437	101.5738	101.6308	101.6649	101.6283
7	143.6529	143.6482	143.6574	143.6501	143.6522
8	99.323	99.3267	99.3269	99.3255	99.3255
9	99.4364	99.4363	99.4361	99.4352	99.436
10	143.2901	143.2748	143.2564	143.2796	143.2752
11	131.2262	131.1696	131.1098	131.1662	131.168
12	136.8662	136.8234	136.8863	136.8295	136.8514
13	139.4395	139.4325	139.4485	139.4311	139.4379
14	111.7744	111.7084	111.8671	111.7696	111.7799
15	129.7872	129.7848	129.748	129.8132	129.7833
16	140.8624	140.8521	140.8947	140.8763	140.8714
17	140.3486	140.3535	140.3039	140.3518	140.3394
18	141.386	141.3645	141.3907	141.4131	141.3886
19	143.3252	143.2759	143.3018	143.3241	143.3068
20	99.6103	99.6059	99.6228	99.6059	99.6112
21	99.4028	99.3777	99.403	99.4159	99.3999
22	99.367	99.3725	99.3837	99.3572	99.3701
23	99.8522	99.8502	99.8808	99.8502	99.8584
24	99.84	99.8274	99.8344	99.8391	99.8352
25	99.2401	99.2293	99.2239	99.2293	99.2307
26	99.7254	99.7246	99.7296	99.7262	99.7264
27	99.6152	99.4545	99.4447	99.4532	99.4919
28	99.7807	99.793	99.7929	99.7914	99.7895
29	99.7682	99.772	99.7733	99.7749	99.7721
30	143.453	143.3554	143.4859	143.4284	143.4307

Table 5.13 VARIANCE VALUES OF WATER

ANGLE-> IMAGE NUMBER	0°	45°	90°	135°	MEAN
1	15.98	15.9808	15.98	15.9803	15.9803
2	26.1275	26.1545	26.1443	26.1363	26.1406
3	24.8704	24.8707	24.8704	24.8707	24.8706
4	25.1112	25.1113	25.1092	25.1059	25.1094
5	35.7653	35.7589	35.7593	35.7662	35.7624
6	26.993	26.9892	26.996	27.0098	26.997
7	35.8082	35.7978	35.8082	35.8081	35.8056
8	25.1011	25.1017	25.0997	25.0971	25.0999
9	25.0187	25.0214	25.02	25.0201	25.02
10	35.7623	35.7672	35.7629	35.7625	35.7637
11	34.2955	34.2903	34.2776	34.287	34.2876
12	35.0814	35.0803	35.086	35.081	35.0822
13	35.4027	35.4049	35.4067	35.4049	35.4048
14	30.2792	30.2761	30.2785	30.2721	30.2765
15	34.0597	34.0085	34.0138	34.052	34.0335
16	35.5417	35.5349	35.5371	35.5396	35.5383
17	35.4992	35.4847	35.4866	35.4981	35.4921
18	35.5683	35.5771	35.5683	35.5664	35.57
19	35.7603	35.7599	35.7603	35.7599	35.7601
20	24.947	24.9431	24.9423	24.9431	24.9439
21	25.2811	25.3026	25.299	25.2845	25.2918
22	25.1496	25.158	25.1555	25.152	25.1538
23	24.8654	24.8661	24.8654	24.8655	24.8656
24	24.8726	24.8728	24.8726	24.8728	24.8727
25	24.7932	24.7911	24.7915	24.7933	24.7923
26	24.8277	24.8281	24.8282	24.8281	24.828
27	25.8251	25.804	25.7979	25.796	25.8058
28	24.8858	24.8795	24.8792	24.8781	24.8807
29	24.8892	24.8895	24.8892	24.8895	24.8893
30	36.9144	36.8977	36.9199	36.923	36.9137

5.3.2 GLCM FEATURES OF URBAN AREA COVERAGE

Table 5.14 ASM VALUES OF URBAN AREA COVERAGE

ANGLE-> IMAGE NUMBER	0°	45°	90°	135°	MEAN
1	0.4039	0.394	0.4016	0.3965	0.399
2	0.2204	0.2206	0.23	0.218	0.2222
3	0.2068	0.193	0.2255	0.2004	0.2064
4	0.186	0.1637	0.1856	0.1664	0.1754
5	0.2131	0.1816	0.201	0.1944	0.1975
6	0.0979	0.0815	0.0935	0.0828	0.0889
7	0.0907	0.0802	0.0872	0.0799	0.0845
8	0.3473	0.3273	0.3496	0.3288	0.3383
9	0.2723	0.2588	0.2765	0.2561	0.2659
10	0.2973	0.2767	0.2995	0.2774	0.2877
11	0.3492	0.3107	0.342	0.315	0.3292
12	0.48	0.4579	0.4802	0.4675	0.4714
13	0.5894	0.5626	0.5823	0.5802	0.5786
14	0.4503	0.4217	0.4477	0.4236	0.4358
15	0.2713	0.2451	0.2739	0.2466	0.2592
16	0.2649	0.2362	0.2609	0.2514	0.2533
17	0.2132	0.1883	0.2195	0.1931	0.2035
18	0.2238	0.1986	0.2227	0.1973	0.2106
19	0.8513	0.8482	0.859	0.8433	0.8505
20	0.6427	0.6216	0.6464	0.6214	0.633
21	0.8536	0.8472	0.8568	0.8411	0.8497
22	0.562	0.5386	0.5622	0.5327	0.5489
23	0.4182	0.3837	0.4092	0.39	0.4003
24	0.3048	0.2816	0.2929	0.274	0.2884
25	0.2855	0.2589	0.2732	0.2512	0.2672
26	0.2526	0.2282	0.2448	0.2207	0.2366
27	0.3334	0.3132	0.3334	0.3133	0.3233
28	0.2463	0.2269	0.2565	0.231	0.2402
29	0.3049	0.2914	0.3646	0.2929	0.3134
30	0.216	0.2015	0.2339	0.2027	0.2135

Table 5.15 CONTRAST VALUES OF URBAN AREA COVERAGE

ANGLE-> IMAGE NUMBER	0°	45°	90°	135°	MEAN
1	0.2918	0.3215	0.3019	0.3245	0.3099
2	0.5646	0.5723	0.4872	0.6201	0.561
3	0.3585	0.4467	0.2909	0.3909	0.3717
4	0.3433	0.4522	0.3423	0.4415	0.3948
5	0.3783	0.5436	0.4188	0.4833	0.456
6	0.7654	1.1815	0.8752	1.1495	0.9929
7	0.8942	1.2505	0.9729	1.3325	1.1125
8	0.3674	0.4598	0.3544	0.442	0.4059
9	0.4087	0.4947	0.3869	0.5028	0.4483
10	0.4082	0.5167	0.3864	0.4905	0.4505
11	0.1963	0.2704	0.2094	0.2597	0.234
12	0.1444	0.1769	0.1429	0.1622	0.1566
13	0.1023	0.1426	0.1108	0.1149	0.1177
14	0.1739	0.2195	0.1776	0.2159	0.1967
15	0.3143	0.4191	0.3106	0.4159	0.3649
16	0.3	0.4273	0.315	0.3514	0.3484
17	0.3302	0.4614	0.3106	0.4203	0.3806
18	0.3496	0.4753	0.3649	0.4827	0.4181
19	0.0477	0.0523	0.0403	0.0576	0.0495
20	0.1133	0.1406	0.1093	0.1409	0.126
21	0.0527	0.0598	0.0497	0.0667	0.0572
22	0.1509	0.1855	0.1512	0.1972	0.1712
23	0.2504	0.3435	0.2685	0.3328	0.2988
24	0.3266	0.4126	0.3772	0.4797	0.399
25	0.3099	0.4044	0.3514	0.4493	0.3788
26	0.3297	0.431	0.3692	0.487	0.4042
27	0.3505	0.43	0.3545	0.4348	0.3924
28	0.3964	0.5142	0.3633	0.4697	0.4359
29	0.3264	0.3676	0.1908	0.3612	0.3115
30	0.4602	0.5734	0.3955	0.558	0.4968

Table 5.16 CORRELATION VALUES OF URBAN AREA COVERAGE

ANGLE-> IMAGE NUMBER	0°	45°	90°	135°	MEAN
1	0.4798	0.4254	0.4605	0.4198	0.4464
2	0.2567	0.2464	0.3576	0.1834	0.261
3	0.672	0.5917	0.7342	0.6427	0.6602
4	0.7369	0.6539	0.7374	0.6621	0.6976
5	0.6139	0.4447	0.5724	0.5063	0.5343
6	0.6596	0.4737	0.6104	0.488	0.5579
7	0.6151	0.4614	0.5816	0.4261	0.5211
8	0.3522	0.1891	0.3752	0.2205	0.2843
9	0.4398	0.321	0.4713	0.3099	0.3855
10	0.4166	0.2611	0.4485	0.2986	0.3562
11	0.7195	0.6139	0.7011	0.6292	0.6659
12	0.6788	0.6067	0.6828	0.6393	0.6519
13	0.7362	0.6315	0.715	0.703	0.6964
14	0.6623	0.5744	0.6554	0.5813	0.6183
15	0.5798	0.4389	0.5846	0.4432	0.5116
16	0.6217	0.4602	0.602	0.5562	0.56
17	0.6969	0.577	0.7155	0.6146	0.651
18	0.6113	0.4711	0.5935	0.4628	0.5347
19	0.5499	0.5016	0.6162	0.4506	0.5296
20	0.5911	0.4927	0.6045	0.4918	0.545
21	0.4722	0.4005	0.5002	0.332	0.4262
22	0.5779	0.4801	0.5754	0.4472	0.5202
23	0.5275	0.352	0.4947	0.3722	0.4366
24	0.5443	0.4248	0.4736	0.3313	0.4435
25	0.551	0.4106	0.4889	0.3451	0.4489
26	0.5815	0.4535	0.5313	0.3825	0.4872
27	0.4165	0.2845	0.4098	0.2765	0.3468
28	0.4869	0.3322	0.5294	0.39	0.4346
29	0.4362	0.3648	0.6705	0.3758	0.4618
30	0.5619	0.4555	0.6248	0.4701	0.5281

Table 5.17 DIFFERENCE ENTROPY VALUES OF URBAN AREA COVERAGE

ANGLE-> IMAGE NUMBER	0°	45°	90°	135°	MEAN
1	0.2679	0.2811	0.2724	0.2826	0.276
2	0.3499	0.3546	0.3315	0.3653	0.3503
3	0.2965	0.3282	0.2677	0.3088	0.3003
4	0.2891	0.327	0.2882	0.324	0.3071
5	0.3004	0.3457	0.3114	0.3348	0.3231
6	0.4084	0.4748	0.4293	0.4708	0.4458
7	0.4307	0.4838	0.4432	0.4961	0.4635
8	0.298	0.3289	0.2928	0.3229	0.3106
9	0.312	0.3392	0.3044	0.3407	0.3241
10	0.3137	0.3464	0.3051	0.3379	0.3258
11	0.2151	0.2547	0.2232	0.2489	0.2355
12	0.1793	0.2027	0.1782	0.1925	0.1882
13	0.1434	0.1782	0.1512	0.1549	0.1569
14	0.2006	0.2288	0.2032	0.2267	0.2148
15	0.2747	0.3137	0.274	0.3132	0.2939
16	0.2679	0.3179	0.2747	0.2901	0.2876
17	0.2829	0.3307	0.2754	0.3162	0.3013
18	0.287	0.3291	0.2948	0.3306	0.3104
19	0.0832	0.0891	0.0733	0.0957	0.0853
20	0.1534	0.1764	0.1498	0.1766	0.164
21	0.0896	0.0983	0.0858	0.1064	0.095
22	0.1844	0.2087	0.1846	0.2165	0.1986
23	0.2475	0.2902	0.2566	0.2862	0.2701
24	0.281	0.3127	0.3015	0.3359	0.3078
25	0.2731	0.3081	0.2901	0.3221	0.2984
26	0.2804	0.3162	0.2975	0.334	0.307
27	0.291	0.3189	0.293	0.3206	0.3059
28	0.3076	0.3435	0.2967	0.329	0.3192
29	0.2801	0.2946	0.2121	0.2921	0.2697
30	0.3289	0.3601	0.3104	0.3551	0.3386

Table 5.18 DIFFERENCE VARIANCE VALUES OF URBAN AREA COVERAGE

ANGLE-> IMAGE NUMBER	0°	45°	90°	135°	MEAN
1	0.2152	0.2316	0.2211	0.2352	0.2258
2	0.3351	0.3426	0.3007	0.3654	0.336
3	0.2527	0.3039	0.2164	0.2715	0.2611
4	0.2397	0.2938	0.238	0.2897	0.2653
5	0.2532	0.3267	0.2689	0.3062	0.2887
6	0.4706	0.6872	0.5316	0.672	0.5903
7	0.5302	0.7254	0.5711	0.7781	0.6512
8	0.251	0.2964	0.2437	0.2867	0.2694
9	0.2707	0.3143	0.2595	0.3175	0.2905
10	0.2747	0.3277	0.261	0.3114	0.2937
11	0.1581	0.1982	0.1659	0.1924	0.1787
12	0.1248	0.1463	0.1237	0.1368	0.1329
13	0.0935	0.1243	0.1001	0.1033	0.1053
14	0.1444	0.1715	0.1467	0.1695	0.158
15	0.2205	0.2719	0.2198	0.2714	0.2459
16	0.2128	0.2787	0.2205	0.2395	0.2379
17	0.2309	0.3007	0.2224	0.2765	0.2576
18	0.2357	0.2962	0.2456	0.2991	0.2692
19	0.0467	0.0509	0.0397	0.0557	0.0483
20	0.102	0.1221	0.099	0.1223	0.1114
21	0.0513	0.0577	0.0485	0.0638	0.0553
22	0.1294	0.1519	0.1295	0.1595	0.1426
23	0.1923	0.2432	0.2021	0.2395	0.2193
24	0.2283	0.2707	0.2555	0.3091	0.2659
25	0.2187	0.2638	0.2395	0.2849	0.2517
26	0.2274	0.2759	0.2495	0.3043	0.2643
27	0.2413	0.2804	0.2442	0.2834	0.2623
28	0.2639	0.3208	0.2493	0.296	0.2825
29	0.227	0.2453	0.1551	0.2421	0.2174
30	0.2963	0.3524	0.2729	0.3424	0.316

Table 5.19 ENTROPY VALUES OF URBAN AREA COVERAGE

ANGLE-> IMAGE NUMBER	0°	45°	90°	135°	MEAN
1	0.6154	0.6257	0.6181	0.6261	0.6213
2	0.7771	0.779	0.7625	0.7835	0.7755
3	0.8227	0.8539	0.7886	0.8357	0.8252
4	0.8701	0.918	0.8697	0.9128	0.8927
5	0.8152	0.8693	0.8315	0.8518	0.8419
6	1.1352	1.2046	1.1578	1.2011	1.1747
7	1.1554	1.2053	1.1696	1.2112	1.1854
8	0.657	0.6775	0.6539	0.6749	0.6658
9	0.7334	0.7549	0.727	0.7567	0.743
10	0.73	0.7558	0.7242	0.7516	0.7404
11	0.6275	0.675	0.6371	0.6687	0.6521
12	0.479	0.5028	0.4784	0.4926	0.4882
13	0.417	0.4502	0.4254	0.428	0.4302
14	0.539	0.5698	0.542	0.5676	0.5546
15	0.7151	0.7553	0.7128	0.7541	0.7343
16	0.7204	0.7711	0.7275	0.7439	0.7407
17	0.8149	0.8679	0.8052	0.8542	0.8356
18	0.7814	0.8261	0.7872	0.8288	0.8059
19	0.1717	0.175	0.1635	0.1796	0.1724
20	0.357	0.3764	0.3532	0.3769	0.3659
21	0.1743	0.1803	0.1712	0.1854	0.1778
22	0.44	0.4617	0.4392	0.4678	0.4522
23	0.5922	0.6304	0.602	0.6258	0.6126
24	0.7076	0.7397	0.7274	0.7561	0.7327
25	0.6883	0.7219	0.7044	0.734	0.7122
26	0.7287	0.7664	0.7445	0.7809	0.7551
27	0.664	0.6861	0.6652	0.6871	0.6756
28	0.743	0.7744	0.7322	0.7647	0.7536
29	0.6232	0.6368	0.5559	0.635	0.6127
30	0.8076	0.8385	0.7905	0.8335	0.8175

Table 5.20 INVERSE DIFFERENCE MOMENT VALUES OF URBAN AREA COVERAGE

ANGLE-> IMAGE NUMBER	0°	45°	90°	135°	MEAN
1	0.864	0.8533	0.8606	0.8545	0.8581
2	0.7588	0.7611	0.7831	0.7488	0.763
3	0.8419	0.8199	0.8664	0.8333	0.8404
4	0.8414	0.8048	0.8403	0.8092	0.8239
5	0.8241	0.766	0.8055	0.7924	0.797
6	0.749	0.6847	0.7327	0.6897	0.714
7	0.7212	0.6766	0.7083	0.6738	0.695
8	0.8316	0.8013	0.8354	0.8056	0.8185
9	0.8166	0.7919	0.8235	0.7886	0.8051
10	0.8216	0.7885	0.8256	0.7923	0.807
11	0.9019	0.8657	0.8955	0.8702	0.8833
12	0.9278	0.9116	0.9285	0.9189	0.9217
13	0.9489	0.93	0.9446	0.9425	0.9415
14	0.9131	0.8904	0.9112	0.8921	0.9017
15	0.8471	0.8089	0.85	0.8111	0.8293
16	0.8523	0.8094	0.8463	0.8333	0.8353
17	0.8437	0.8046	0.8532	0.813	0.8286
18	0.8304	0.7881	0.8277	0.785	0.8078
19	0.9762	0.9739	0.9799	0.9712	0.9753
20	0.9434	0.9297	0.9454	0.9296	0.937
21	0.9737	0.9701	0.9752	0.9667	0.9714
22	0.9248	0.9077	0.9245	0.9027	0.9149
23	0.881	0.8452	0.873	0.8514	0.8626
24	0.8442	0.8133	0.8279	0.7986	0.821
25	0.8493	0.8126	0.8334	0.7974	0.8231
26	0.8398	0.8029	0.8282	0.7874	0.8146
27	0.8363	0.8089	0.836	0.8081	0.8223
28	0.8199	0.7834	0.8335	0.7925	0.8073
29	0.8428	0.8247	0.9051	0.8269	0.8499
30	0.8009	0.7708	0.8307	0.772	0.7936

Table 5.21 INFORMATION MEASURE OF CORRELATION 1 OF URBAN AREA COVERAGE

ANGLE-> IMAGE NUMBER	0°	45°	90°	135°	MEAN
1	-2.7552	-2.7155	-2.7455	-2.7257	-2.7355
2	-2.6456	-2.6381	-2.6781	-2.6258	-2.6469
3	-2.8802	-2.815	-2.954	-2.8536	-2.8757
4	-2.9337	-2.8408	-2.9326	-2.8522	-2.8898
5	-2.8294	-2.7107	-2.794	-2.7497	-2.771
6	-2.8119	-2.6991	-2.7757	-2.7092	-2.749
7	-2.7714	-2.692	-2.7497	-2.6823	-2.7239
8	-2.692	-2.6304	-2.7015	-2.6419	-2.6665
9	-2.7241	-2.6651	-2.7394	-2.6601	-2.6972
10	-2.7101	-2.6407	-2.7294	-2.6563	-2.6842
11	-2.9835	-2.861	-2.9605	-2.8784	-2.9209
12	-2.9756	-2.8916	-2.9754	-2.9241	-2.9417
13	-3.0571	-2.9325	-3.035	-3.0145	-3.0098
14	-2.944	-2.8538	-2.936	-2.855	-2.8972
15	-2.8224	-2.7223	-2.8278	-2.7226	-2.7738
16	-2.8524	-2.729	-2.8382	-2.7933	-2.8032
17	-2.9009	-2.7916	-2.924	-2.8201	-2.8592
18	-2.834	-2.7316	-2.8183	-2.7246	-2.7771
19	-2.9085	-2.8575	-2.984	-2.8236	-2.8934
20	-2.9082	-2.8137	-2.9249	-2.8195	-2.8666
21	-2.8579	-2.7974	-2.8824	-2.7461	-2.821
22	-2.8847	-2.7869	-2.8752	-2.7692	-2.829
23	-2.8021	-2.6844	-2.7811	-2.7028	-2.7426
24	-2.794	-2.7129	-2.7445	-2.6718	-2.7308
25	-2.8037	-2.7038	-2.7534	-2.6756	-2.7341
26	-2.8172	-2.7258	-2.7796	-2.6908	-2.7533
27	-2.7209	-2.6585	-2.7173	-2.6557	-2.6881
28	-2.7478	-2.6626	-2.7747	-2.6935	-2.7196
29	-2.7331	-2.6905	-2.9361	-2.698	-2.7644
30	-2.7884	-2.7241	-2.8305	-2.7297	-2.7682

Table 5.22 INFORMATION MEASURE OF CORRELATION 2 OF URBAN AREA COVERAGE

ANGLE-> IMAGE NUMBER	0°	45°	90°	135°	MEAN
1	0.9177	0.9154	0.9167	0.9153	0.9163
2	0.9367	0.9365	0.9385	0.9359	0.9369
3	0.9676	0.9655	0.9698	0.9667	0.9674
4	0.9762	0.9738	0.9762	0.9741	0.9751
5	0.9621	0.9576	0.9608	0.9591	0.9599
6	0.9858	0.9836	0.9851	0.9837	0.9846
7	0.9847	0.9831	0.9843	0.9829	0.9837
8	0.9182	0.9146	0.9188	0.9151	0.9167
9	0.9384	0.9354	0.9394	0.9352	0.9371
10	0.9366	0.9331	0.9376	0.9337	0.9353
11	0.9492	0.944	0.9483	0.9448	0.9466
12	0.9091	0.9045	0.9096	0.9065	0.9074
13	0.8996	0.8919	0.8983	0.8969	0.8967
14	0.9235	0.9186	0.9231	0.919	0.921
15	0.9468	0.9421	0.947	0.9422	0.9445
16	0.9514	0.9459	0.9506	0.9489	0.9492
17	0.9683	0.9648	0.9691	0.9658	0.967
18	0.9581	0.954	0.9575	0.9538	0.9559
19	0.6703	0.6646	0.674	0.6607	0.6674
20	0.8414	0.8348	0.8421	0.8345	0.8382
21	0.6593	0.6541	0.6605	0.6495	0.6559
22	0.8788	0.8726	0.8783	0.871	0.8752
23	0.9184	0.9116	0.9171	0.9125	0.9149
24	0.9421	0.9383	0.9397	0.9362	0.9391
25	0.9397	0.9345	0.9371	0.9328	0.936
26	0.9485	0.9445	0.9468	0.9428	0.9457
27	0.9236	0.9201	0.9235	0.9199	0.9218
28	0.9433	0.9392	0.9446	0.9404	0.9419
29	0.9157	0.9131	0.9268	0.9135	0.9173
30	0.9576	0.955	0.9593	0.9555	0.9569

Table 5.23 SUM AVERAGE VALUES OF URBAN AREA COVERAGE

ANGLE-> IMAGE NUMBER	0°	45°	90°	135°	MEAN
1	11.716	11.7161	11.7146	11.7162	11.7157
2	11.118	11.1184	11.1191	11.1184	11.1185
3	9.465	9.4663	9.4674	9.4664	9.4663
4	9.0987	9.0953	9.0927	9.0953	9.0955
5	8.466	8.4641	8.4641	8.4641	8.4645
6	10.4758	10.4764	10.4726	10.4766	10.4754
7	10.8694	10.8704	10.8728	10.8707	10.8708
8	10.108	10.1089	10.1078	10.1088	10.1084
9	10.2867	10.2878	10.285	10.2877	10.2868
10	9.8232	9.8225	9.8207	9.8224	9.8222
11	12.1156	12.1161	12.1166	12.1161	12.1161
12	12.3853	12.3849	12.3866	12.3849	12.3854
13	12.072	12.0734	12.072	12.0734	12.0727
14	12.091	12.0902	12.0885	12.0902	12.09
15	11.6962	11.694	11.6937	11.694	11.6944
16	12.1673	12.1684	12.1667	12.1684	12.1677
17	11.0131	11.0154	11.0219	11.0154	11.0164
18	10.8699	10.871	10.8726	10.871	10.8712
19	12.0735	12.0731	12.0733	12.073	12.0732
20	12.1997	12.1996	12.1994	12.1996	12.1996
21	12.0434	12.0431	12.0431	12.0431	12.0432
22	12.1499	12.1505	12.151	12.1506	12.1505
23	11.8804	11.8795	11.8804	11.8795	11.8799
24	11.687	11.686	11.6834	11.686	11.6856
25	11.2948	11.2909	11.2895	11.2908	11.2915
26	11.0803	11.079	11.0803	11.079	11.0797
27	12.2306	12.2321	12.2324	12.2321	12.2318
28	11.0985	11.1024	11.1002	11.1024	11.1009
29	11.1916	11.1928	11.1904	11.1929	11.1919
30	10.9418	10.9406	10.9426	10.9405	10.9414

Table 5.24 SUM ENTROPY VALUES OF URBAN AREA COVERAGE

ANGLE-> IMAGE NUMBER	0°	45°	90°	135°	MEAN
1	0.5175	0.5163	0.5162	0.5142	0.5161
2	0.5884	0.5883	0.6	0.5763	0.5882
3	0.6985	0.6972	0.6901	0.6989	0.6962
4	0.7543	0.7607	0.7552	0.7594	0.7574
5	0.6893	0.6843	0.6924	0.6856	0.6879
6	0.8829	0.8659	0.8792	0.8678	0.874
7	0.8786	0.8633	0.8764	0.8579	0.8691
8	0.5322	0.5178	0.5349	0.5226	0.5269
9	0.5959	0.5859	0.5979	0.5867	0.5916
10	0.5881	0.5756	0.5919	0.5813	0.5842
11	0.5684	0.592	0.5735	0.5903	0.581
12	0.4356	0.4496	0.4353	0.4438	0.4411
13	0.3862	0.405	0.3921	0.3934	0.3942
14	0.4867	0.5034	0.4885	0.5024	0.4952
15	0.615	0.6139	0.6128	0.6133	0.6138
16	0.6266	0.6254	0.6278	0.6288	0.6271
17	0.7062	0.7077	0.7025	0.7109	0.7068
18	0.6697	0.6663	0.6672	0.6652	0.6671
19	0.1573	0.1591	0.1514	0.1622	0.1575
20	0.3229	0.334	0.3203	0.3345	0.3279
21	0.1585	0.1623	0.1562	0.1653	0.1606
22	0.394	0.405	0.3935	0.4061	0.3997
23	0.5094	0.5116	0.5125	0.51	0.5108
24	0.601	0.5992	0.5991	0.5887	0.597
25	0.5892	0.5863	0.5885	0.581	0.5863
26	0.6233	0.6211	0.6204	0.6135	0.6196
27	0.5487	0.5415	0.547	0.5398	0.5443
28	0.6089	0.5979	0.6091	0.6054	0.6053
29	0.5192	0.5188	0.4975	0.5197	0.5138
30	0.6542	0.6516	0.6559	0.6499	0.6529

Table 5.25 SUM VARIANCE VALUES OF URBAN AREA COVERAGE

ANGLE-> IMAGE NUMBER	0°	45°	90°	135°	MEAN
1	126.2349	126.2336	126.2198	126.2806	126.2422
2	111.8264	111.8304	111.6821	112.0344	111.8433
3	78.6797	78.6385	78.9403	78.6671	78.7314
4	71.8945	71.6266	71.7789	71.6592	71.7398
5	62.0581	61.9387	61.9394	61.9792	61.9789
6	95.7548	95.67	95.6526	95.6704	95.6869
7	103.5672	103.5367	103.6054	103.5677	103.5692
8	92.4623	92.6631	92.4203	92.5866	92.5331
9	94.9618	95.0888	94.9159	95.0635	95.0075
10	86.2782	86.3879	86.1863	86.3071	86.2899
11	134.5418	133.9358	134.4363	133.9866	134.2251
12	143.5509	143.1742	143.5914	143.3261	143.4106
13	137.2309	136.7835	137.0879	137.0809	137.0458
14	135.5167	135.0672	135.4124	135.0923	135.2722
15	123.9735	123.8433	123.9699	123.8585	123.9113
16	134.474	134.3969	134.4141	134.394	134.4198
17	108.0814	107.9684	108.3637	107.9428	108.0891
18	105.4927	105.4592	105.5813	105.4727	105.5015
19	142.1585	142.1001	142.3026	142.0187	142.145
20	141.5003	141.2053	141.5554	141.1936	141.3637
21	141.3972	141.2937	141.4468	141.2142	141.338
22	138.7649	138.483	138.7993	138.4488	138.624
23	130.1095	129.9471	130.0235	129.9926	130.0182
24	124.007	123.9389	123.9166	124.1035	123.9915
25	115.6789	115.5552	115.5353	115.6221	115.5979
26	110.5954	110.5138	110.615	110.6174	110.5854
27	137.3182	137.4419	137.3937	137.4778	137.4079
28	111.1809	111.3686	111.244	111.2587	111.2631
29	114.7331	114.7238	115.3051	114.7118	114.8684
30	107.4756	107.3957	107.5291	107.4445	107.4612

Table 5.26 VARIANCE VALUES OF URBAN AREA COVERAGE

ANGLE-> IMAGE NUMBER	0°	45°	90°	135°	MEAN
1	34.4002	34.4443	34.4217	34.418	34.4211
2	31.1119	31.1147	31.1211	31.1207	31.1171
3	22.8061	22.7817	22.7981	22.8031	22.7972
4	21.2072	21.2088	21.1956	21.2095	21.2053
5	18.291	18.2518	18.2674	18.2821	18.2731
6	28.3782	28.4515	28.4141	28.4153	28.4148
7	30.5317	30.5188	30.5368	30.5273	30.5287
8	25.6863	25.6445	25.6566	25.6788	25.6665
9	26.6623	26.663	26.6546	26.6705	26.6626
10	24.3313	24.2943	24.2975	24.3161	24.3098
11	36.871	36.8421	36.8585	36.8686	36.86
12	38.3682	38.382	38.381	38.3575	38.3722
13	36.4281	36.4623	36.4441	36.4413	36.4439
14	36.6272	36.5956	36.5953	36.6161	36.6085
15	34.3886	34.3719	34.368	34.3667	34.3738
16	37.204	37.215	37.191	37.1877	37.1994
17	30.7037	30.694	30.7385	30.7109	30.7118
18	29.8069	29.8477	29.8444	29.8243	29.8308
19	36.3016	36.3098	36.3067	36.2995	36.3044
20	37.1635	37.1468	37.1522	37.1611	37.1559
21	36.1226	36.1224	36.1224	36.1224	36.1225
22	36.8949	36.8951	36.8985	36.8968	36.8963
23	35.371	35.3469	35.3583	35.358	35.3586
24	34.3214	34.3153	34.2984	34.3125	34.3119
25	32.0705	32.071	32.0726	32.088	32.0755
26	30.93	30.8909	30.9136	30.9226	30.9143
27	37.5036	37.5133	37.5118	37.5074	37.509
28	30.9988	31.0233	31.0042	31.0066	31.0082
29	31.4181	31.4465	31.4236	31.4274	31.4289
30	30.2878	30.2934	30.3078	30.2979	30.2967

5.3.3 GLRLM FEATURES OF WATER COVERAGE

Table 5.27 GLRLM Features of WATER

IMAGE NO	SRE	LRE	GLN	RP	RLN	LGRE	HGRE
1	0.8969	1.5552	1327.2	0.861	10950.5	0.0001	912357
2	0.9297	1.3222	565.433	0.9082	12467.3	0.0001	251462
3	0.9362	1.2971	948.07	0.9154	12881.2	0.0002	174183
4	0.9302	1.3243	941.128	0.9082	12580.8	0.0003	120162
5	0.8971	1.5374	859.08	0.8629	10979.2	0.0001	697795
6	0.9035	1.4908	777.137	0.8721	11016.1	0.0006	99197.1
7	0.8961	1.5478	828.113	0.8612	10928	0.0001	753629
8	0.9126	1.427	1324.16	0.8852	11716.8	0.0002	59491.7
9	0.9119	1.4396	1296.93	0.883	11668.3	0.0003	47861.5
10	0.9393	1.278	830.692	0.9198	13046.5	0.0001	181956
11	0.9424	1.2646	675.095	0.9234	13207.5	0.0003	139876
12	0.9397	1.2726	826.905	0.9209	13074.5	0.0001	389443
13	0.9375	1.2817	768.444	0.9183	12962.1	0.0001	280769
14	0.8441	1.9271	1242.34	0.7951	8824.83	0.0005	36342.5
15	0.8303	2.0583	1699.2	0.7767	8318.26	0.0001	70827.2
16	0.8303	2.0575	1259.81	0.777	8321.38	0.0001	59346.6
17	0.8263	2.1027	1668.53	0.771	8171.49	0.0005	19270.4
18	0.8294	2.0447	1571.9	0.7776	8309.53	0.0001	243169
19	0.8233	2.1327	1404.02	0.7664	8060.68	0.0001	68114
20	0.8891	1.593	733.545	0.8526	10625.9	0.0004	125838
21	0.8855	1.6143	1128.62	0.8483	10474.1	0.0001	80711.1
22	0.8828	1.6312	1004.75	0.8448	10358.7	0.0001	91038.6
23	0.9102	1.4522	1160.94	0.8806	11588.5	0.0001	183924
24	0.9151	1.4191	1427.52	0.8874	11824.5	0.0002	164246
25	0.9466	1.2454	924.089	0.9287	13427.4	0.0001	1460933
26	0.9402	1.271	812.136	0.9213	13099.1	0.0001	280144
27	0.9187	1.3897	859.486	0.8931	12011.2	0.0004	62212
28	0.8569	1.8226	1687.99	0.8113	9306.46	0.0005	52293.4
29	0.867	1.7412	1418.98	0.825	9711.49	0.0001	75443
30	0.8104	2.2694	1599.59	0.7493	7621.36	0.0001	1388667
MEAN	0.89264	1.59368	1119.06	0.85819	10917.8	0.00021	285690
STDEV	0.0429	0.31386	337.572	0.05638	1840.79	0.00016	378950

5.3.4 GLRLM FEATURES OF URBAN AREA COVERAGE

Table 5.28 GLRLM Features of Urban Area

IMAGE NO	SRE	LRE	GLN	RP	RLN	LGRE	HGRE
1	0.977	1.0973	287.526	0.9694	15179.6	0.0003	1712003.7
2	0.9893	1.0443	234.843	0.9856	15940.5	0.0003	1658203.9
3	0.9754	1.1049	182.25	0.9671	15080.5	0.0004	1237038.4
4	0.9733	1.1151	167.43	0.9642	14950.4	0.0003	1288753
5	0.9785	1.0914	205.757	0.9712	15267.2	0.0005	930621
6	0.9781	1.0922	123.771	0.9709	15244.4	0.0003	5209877.7
7	0.9852	1.0625	123.803	0.9801	15682.2	0.0003	3982423
8	0.975	1.1081	311.058	0.9664	15051.7	0.0002	1622135.5
9	0.9755	1.1034	295.07	0.9674	15085.8	0.0004	2776267.2
10	0.9784	1.0895	252.422	0.9715	15264	0.0003	1541237.3
11	0.9554	1.1968	249.165	0.941	13920.8	0.0003	1023269.3
12	0.9576	1.1854	309.136	0.9439	14044.6	0.0003	664711.82
13	0.9521	1.2159	331.227	0.9362	13732	0.0003	1249400.5
14	0.957	1.1866	281.248	0.9434	14012.8	0.0003	732075.85
15	0.9765	1.1	223.761	0.9686	15144	0.0003	1227494.7
16	0.9738	1.1094	233.799	0.9654	14985.8	0.0003	1486374.8
17	0.9759	1.1033	183.957	0.9677	15111.1	0.0003	1111204.7
18	0.9791	1.088	205.537	0.9721	15305	0.0004	905745.82
19	0.9432	1.2576	462.442	0.925	13252.7	0.0004	338562.85
20	0.9544	1.2019	372.506	0.9396	13863.9	0.0003	608569.9
21	0.9478	1.2369	453.827	0.9306	13496.9	0.0003	489044.98
22	0.96	1.1742	338.65	0.9471	14182.1	0.0004	625964.08
23	0.97	1.1316	282.463	0.9597	14751.7	0.0003	1701683.6
24	0.9761	1.1005	233.164	0.9683	15122.4	0.0004	1414567.3
25	0.9772	1.0949	238.038	0.9699	15194.6	0.0001	2241437.2
26	0.9779	1.0925	226.876	0.9707	15233.9	0.0002	1173928.3
27	0.9709	1.1284	323.242	0.9606	14802.4	0.0003	1769557.4
28	0.9816	1.0769	225.418	0.9755	15459.8	0.0003	1332122.4
29	0.9781	1.0917	297.645	0.9709	15245.4	0.0003	1185079.2
30	0.9793	1.0892	206.549	0.9721	15315	0.0002	1471948.2
MEAN	0.97099	1.12568	262.086	0.9614	14830.8	0.00031	1490376.8
STDEV	0.01167	0.05421	80.5783	0.01538	679.258	7.6E-05	1001152.3

After each parameter is calculated in all the four directions, mean of all the 4 directions for each image has been found. This mean is being shown in the last column of each of the tables shown above. Then all the means are combined in one table to form the final training set using GLCM. Similarly, 7 GLRLM features are tabulated in one table. The final training matrix of water and urban area coverage is of dimensions 30×20. This final matrix contains all the 20 texture features.

Table 5.29 TRAINING SET OF WATER

IMAGE NO	ASM	CON	CORR	D_ENT	D_VAR	ENT	IDM	IMCORR 1	IMCORR 2	S_AVG	S_ENT	S_VAR	VAR	SRE	LRE	GLN	RP	RLN	LGRE	HGRE
1	0.9643	0.017	0.3917	0.0353	0.0171	0.0504	0.9922	-2.7775	0.3778	8.0228	0.0453	63.6794	15.9803	0.8969	1.5552	1327.2	0.861	10950.5	0.0001	912357
2	0.7314	0.0641	0.693	0.1034	0.0615	0.248	0.968	-3.0247	0.7856	10.2363	0.2287	100.505	26.1406	0.9297	1.3222	565.433	0.9082	12467.3	0.0001	251462
3	0.9935	0.004	0.4388	0.0092	0.004	0.0118	0.9985	-2.8069	0.19	10.0046	0.0109	99.8845	24.8706	0.9362	1.2971	948.07	0.9154	12881.2	0.0002	174183
4	0.9195	0.0392	0.2442	0.0708	0.0388	0.0955	0.9811	-2.6624	0.4845	10.0486	0.0836	99.3664	25.1094	0.9302	1.3243	941.128	0.9082	12580.8	0.0003	120162
5	0.9818	0.0086	0.1534	0.0214	0.0087	0.0268	0.9958	-2.5636	0.2676	11.9905	0.0243	143.202	35.7624	0.8971	1.5374	859.08	0.8629	10979.2	0.0001	697795
6	0.5595	0.148	0.5299	0.182	0.1272	0.3785	0.926	-2.8364	0.8398	10.3911	0.3339	101.628	26.997	0.9035	1.4908	777.137	0.8721	11016.1	0.0006	99197.1
7	0.992	0.0038	0.1968	0.0106	0.0038	0.0139	0.9982	-2.5326	0.1991	11.9982	0.013	143.652	35.8056	0.8961	1.5478	828.113	0.8612	10928	0.0001	753629
8	0.9106	0.0454	0.0154	0.0802	0.0445	0.097	0.9774	-2.5845	0.4727	10.0472	0.0833	99.3255	25.0999	0.9126	1.427	1324.16	0.8852	11716.8	0.0002	59491.7
9	0.9399	0.0294	0.0666	0.0576	0.0294	0.0708	0.9853	-2.6113	0.4128	10.032	0.062	99.436	25.02	0.9119	1.4396	1296.93	0.883	11668.3	0.0003	47861.5
10	0.9834	0.0078	0.1193	0.0198	0.0079	0.0241	0.9961	-2.5754	0.252	11.9911	0.0218	143.275	35.7637	0.9393	1.278	830.692	0.9198	13046.5	0.0001	181956
11	0.6222	0.1672	0.2993	0.196	0.14	0.3341	0.9164	-2.6852	0.7807	11.7231	0.2838	131.168	34.2876	0.9424	1.2646	675.095	0.9234	13207.5	0.0003	139876
12	0.796	0.0872	0.2994	0.1285	0.0812	0.2015	0.9564	-2.7092	0.662	11.8667	0.1752	136.851	35.0822	0.9397	1.2726	826.905	0.9209	13074.5	0.0001	389443
13	0.8643	0.0673	0.0793	0.107	0.0643	0.1403	0.9664	-2.6098	0.5564	11.9251	0.1201	139.438	35.4048	0.9375	1.2817	768.444	0.9183	12962.1	0.0001	280769
14	0.3421	0.1966	0.6067	0.2152	0.1583	0.5162	0.9017	-2.8902	0.908	10.9916	0.457	111.78	30.2765	0.8441	1.9271	1242.34	0.7951	8824.83	0.0005	36342.5
15	0.6103	0.1373	0.4937	0.1738	0.1198	0.3433	0.9313	-2.8015	0.8134	11.6764	0.302	129.783	34.0335	0.8303	2.0583	1699.2	0.7767	8318.26	0.0001	70827.2
16	0.9196	0.0329	0.3238	0.0628	0.0327	0.0938	0.9836	-2.7362	0.4934	11.9501	0.0839	140.871	35.5383	0.8303	2.0575	1259.81	0.777	8321.38	0.0001	59346.6
17	0.8974	0.0482	0.1514	0.0839	0.0471	0.1123	0.9759	-2.614	0.5119	11.9415	0.0978	140.339	35.4921	0.8263	2.1027	1668.53	0.771	8171.49	0.0005	19270.4
18	0.9401	0.0175	0.5907	0.0383	0.0176	0.0737	0.9913	-2.9469	0.4889	11.9563	0.0685	141.389	35.57	0.8294	2.0447	1571.9	0.7776	8309.53	0.0001	243169
19	0.9862	0.0043	0.5548	0.0119	0.0043	0.0212	0.9979	-3	0.2761	11.9904	0.0199	143.307	35.7601	0.8233	2.1327	1404.02	0.7664	8060.68	0.0001	68114
20	0.9675	0.0143	0.2192	0.0326	0.0145	0.0434	0.9928	-2.6669	0.3409	10.0185	0.0391	99.6112	24.9439	0.8891	1.593	733.545	0.8526	10625.9	0.0004	125838
21	0.8819	0.0417	0.4664	0.0753	0.0411	0.1298	0.9791	-2.8133	0.5864	10.0815	0.1173	99.3999	25.2918	0.8855	1.6143	1128.62	0.8483	10474.1	0.0001	80711.1
22	0.9114	0.0354	0.3491	0.0665	0.0352	0.1019	0.9823	-2.741	0.5143	10.056	0.0913	99.3701	25.1538	0.8828	1.6312	1004.75	0.8448	10358.7	0.0001	91038.6
23	0.9925	0.0035	0.1532	0.01	0.0035	0.0123	0.9983	-2.8434	0.1852	10.0039	0.0113	99.8584	24.8656	0.9102	1.4522	1160.94	0.8806	11588.5	0.0001	183924
24	0.9905	0.0043	0.1723	0.0121	0.0044	0.0151	0.9978	-2.6933	0.2039	10.0052	0.0138	99.8352	24.8727	0.9151	1.4191	1427.52	0.8874	11824.5	0.0002	164246
25	0.9779	0.0114	0.0545	0.0264	0.0116	0.0309	0.9945	-2.5859	0.28	9.9883	0.0275	99.2307	24.7923	0.9466	1.2454	924.089	0.9287	13427.4	0.0001	1460933
26	0.9931	0.0034	0.0657	0.0098	0.0034	0.0113	0.9983	-2.605	0.1723	9.9964	0.0103	99.7264	24.828	0.9402	1.271	812.136	0.9213	13099.1	0.0001	280144
27	0.7335	0.1184	0.2697	0.1576	0.1058	0.2495	0.9408	-2.6648	0.7102	10.1781	0.2139	99.4919	25.8058	0.9187	1.3897	859.486	0.8931	12011.2	0.0004	62212
28	0.9868	0.006	0.1611	0.016	0.0061	0.02	0.997	-2.5301	0.2325	10.0072	0.0182	99.7895	24.8807	0.8569	1.8226	1687.99	0.8113	9306.46	0.0005	52293.4
29	0.9853	0.0068	0.1379	0.0177	0.0069	0.0219	0.9966	-2.58	0.2414	10.0079	0.0198	99.7721	24.8893	0.867	1.7412	1418.98	0.825	9711.49	0.0001	75443
30	0.7649	0.0877	0.4375	0.129	0.0817	0.2286	0.9563	-2.7838	0.7127	12.1692	0.2023	143.431	36.9137	0.8104	2.2694	1599.59	0.7493	7621.36	0.0001	1388667
MEAN	0.87131	0.04862	0.29116	0.07202	0.04408	0.12393	0.97578	-2.71586	0.465083	10.7765	0.10933	114.947	29.1744	0.89264	1.59368	1119.06	0.85819	10917.8	0.00021	285690
STDEV	0.16059	0.05461	0.18969	0.06297	0.0459	0.13146	0.02735	0.1368456	0.228403	1.0507	0.11537	21.9333	5.60004	0.0429	0.31386	337.572	0.05638	1840.79	0.00016	378950

Table 5.30 TRAINING SET OF URBAN AREA

IMAGE NO	ASM	CON	CORR	D_ENT	D_VAR	ENT	IDM	IMCORR 1	IMCORR 2	S_AVG	S_ENT	S_VAR	VAR	SRE	LRE	GLN	RP	RLN	LGRE	HGRE
1	0.399	0.3099	0.4464	0.276	0.2258	0.6213	0.8581	-2.7355	0.9163	11.7157	0.5161	126.242	34.4211	0.977	1.0973	287.526	0.9694	15179.6	0.0003	1712003.7
2	0.2222	0.561	0.261	0.3503	0.336	0.7755	0.763	-2.6469	0.9369	11.1185	0.5882	111.843	31.1171	0.9893	1.0443	234.843	0.9856	15940.5	0.0003	1658203.9
3	0.2064	0.3717	0.6602	0.3003	0.2611	0.8252	0.8404	-2.8757	0.9674	9.4663	0.6962	78.7314	22.7972	0.9754	1.1049	182.25	0.9671	15080.5	0.0004	1237038.4
4	0.1754	0.3948	0.6976	0.3071	0.2653	0.8927	0.8239	-2.8898	0.9751	9.0955	0.7574	71.7398	21.2053	0.9733	1.1151	167.43	0.9642	14950.4	0.0003	1288753
5	0.1975	0.456	0.5343	0.3231	0.2887	0.8419	0.797	-2.771	0.9599	8.4645	0.6879	61.9789	18.2731	0.9785	1.0914	205.757	0.9712	15267.2	0.0005	930621
6	0.0889	0.9929	0.5579	0.4458	0.5903	1.1747	0.714	-2.749	0.9846	10.4754	0.874	95.6869	28.4148	0.9781	1.0922	123.771	0.9709	15244.4	0.0003	5209877.7
7	0.0845	1.1125	0.5211	0.4635	0.6512	1.1854	0.695	-2.7239	0.9837	10.8708	0.8691	103.569	30.5287	0.9852	1.0625	123.803	0.9801	15682.2	0.0003	3982423
8	0.3383	0.4059	0.2843	0.3106	0.2694	0.6658	0.8185	-2.6665	0.9167	10.1084	0.5269	92.5331	25.6665	0.975	1.1081	311.058	0.9664	15051.7	0.0002	1622135.5
9	0.2659	0.4483	0.3855	0.3241	0.2905	0.743	0.8051	-2.6972	0.9371	10.2868	0.5916	95.0075	26.6626	0.9755	1.1034	295.07	0.9674	15085.8	0.0004	2776267.2
10	0.2877	0.4505	0.3562	0.3258	0.2937	0.7404	0.807	-2.6842	0.9353	9.8222	0.5842	86.2899	24.3098	0.9784	1.0895	252.422	0.9715	15264	0.0003	1541237.3
11	0.3292	0.234	0.6659	0.2355	0.1787	0.6521	0.8833	-2.9209	0.9466	12.1161	0.581	134.225	36.86	0.9554	1.1968	249.165	0.941	13920.8	0.0003	1023269.3
12	0.4714	0.1566	0.6519	0.1882	0.1329	0.4882	0.9217	-2.9417	0.9074	12.3854	0.4411	143.411	38.3722	0.9576	1.1854	309.136	0.9439	14044.6	0.0003	664711.82
13	0.5786	0.1177	0.6964	0.1569	0.1053	0.4302	0.9415	-3.0098	0.8967	12.0727	0.3942	137.046	36.4439	0.9521	1.2159	331.227	0.9362	13732	0.0003	1249400.5
14	0.4358	0.1967	0.6183	0.2148	0.158	0.5546	0.9017	-2.8972	0.921	12.09	0.4952	135.272	36.6085	0.957	1.1866	281.248	0.9434	14012.8	0.0003	732075.85
15	0.2592	0.3649	0.5116	0.2939	0.2459	0.7343	0.8293	-2.7738	0.9445	11.6944	0.6138	123.911	34.3738	0.9765	1.1	223.761	0.9686	15144	0.0003	1227494.7
16	0.2533	0.3484	0.56	0.2876	0.2379	0.7407	0.8353	-2.8032	0.9492	12.1677	0.6271	134.42	37.1994	0.9738	1.1094	233.799	0.9654	14985.8	0.0003	1486374.8
17	0.2035	0.3806	0.651	0.3013	0.2576	0.8356	0.8286	-2.8592	0.967	11.0164	0.7068	108.089	30.7118	0.9759	1.1033	183.957	0.9677	15111.1	0.0003	1111204.7
18	0.2106	0.4181	0.5347	0.3104	0.2692	0.8059	0.8078	-2.7771	0.9559	10.8712	0.6671	105.502	29.8308	0.9791	1.088	205.537	0.9721	15305	0.0004	905745.82
19	0.8505	0.0495	0.5296	0.0853	0.0483	0.1724	0.9753	-2.8934	0.6674	12.0732	0.1575	142.145	36.3044	0.9432	1.2576	462.442	0.925	13252.7	0.0004	338562.85
20	0.633	0.126	0.545	0.164	0.1114	0.3659	0.937	-2.8666	0.8382	12.1996	0.3279	141.364	37.1559	0.9544	1.2019	372.506	0.9396	13863.9	0.0003	608569.9
21	0.8497	0.0572	0.4262	0.095	0.0553	0.1778	0.9714	-2.821	0.6559	12.0432	0.1606	141.338	36.1225	0.9478	1.2369	453.827	0.9306	13496.9	0.0003	489044.98
22	0.5489	0.1712	0.5202	0.1986	0.1426	0.4522	0.9149	-2.829	0.8752	12.1505	0.3997	138.624	36.8963	0.96	1.1742	338.65	0.9471	14182.1	0.0004	625964.08
23	0.4003	0.2988	0.4366	0.2701	0.2193	0.6126	0.8626	-2.7426	0.9149	11.8799	0.5108	130.018	35.3586	0.97	1.1316	282.463	0.9597	14751.7	0.0003	1701683.6
24	0.2884	0.399	0.4435	0.3078	0.2659	0.7327	0.821	-2.7308	0.9391	11.6856	0.597	123.992	34.3119	0.9761	1.1005	233.164	0.9683	15122.4	0.0004	1414567.3
25	0.2672	0.3788	0.4489	0.2984	0.2517	0.7122	0.8231	-2.7341	0.936	11.2915	0.5863	115.598	32.0755	0.9772	1.0949	238.038	0.9699	15194.6	0.0001	2241437.2
26	0.2366	0.4042	0.4872	0.307	0.2643	0.7551	0.8146	-2.7533	0.9457	11.0797	0.6196	110.585	30.9143	0.9779	1.0925	226.876	0.9707	15233.9	0.0002	1173928.3
27	0.3233	0.3924	0.3468	0.3059	0.2623	0.6756	0.8223	-2.6881	0.9218	12.2318	0.5443	137.408	37.509	0.9709	1.1284	323.242	0.9606	14802.4	0.0003	1769557.4
28	0.2402	0.4359	0.4346	0.3192	0.2825	0.7536	0.8073	-2.7196	0.9419	11.1009	0.6053	111.263	31.0082	0.9816	1.0769	225.418	0.9755	15459.8	0.0003	1332122.4
29	0.3134	0.3115	0.4618	0.2697	0.2174	0.6127	0.8499	-2.7644	0.9173	11.1919	0.5138	114.868	31.4289	0.9781	1.0917	297.645	0.9709	15245.4	0.0003	1185079.2
30	0.2135	0.4968	0.5281	0.3386	0.316	0.8175	0.7936	-2.7682	0.9569	10.9414	0.6529	107.461	30.2967	0.9793	1.0892	206.549	0.9721	15315	0.0002	1471948.2
MEAN	0.33908	0.37473	0.50676	0.27916	0.24982	0.68493	0.84214	-2.791123	0.9170533	11.1902	0.56312	115.339	31.7726	0.97099	1.12568	262.086	0.9614	14830.8	0.00031	1490376.8
STDEV	0.19039	0.22685	0.11571	0.08416	0.12549	0.22576	0.06641	0.0896855	0.075989	1.01885	0.16421	22.4488	5.31811	0.01167	0.05421	80.5783	0.01538	679.258	7.6E-05	1001152.3

5.4. BOXPLOTS:

A box plot or a box and whisker diagram provides a simple graphical summary of a set of data. Box plots are especially useful when comparing two or more sets of data.

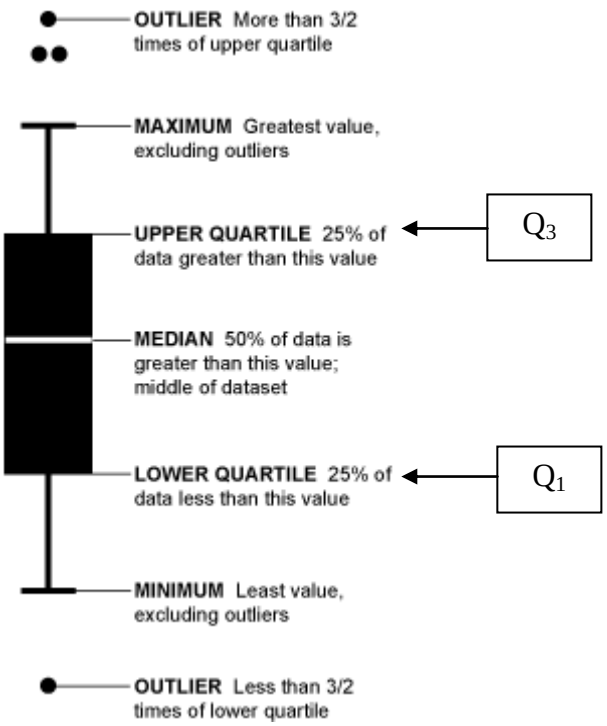

Figure 5.11 A general Box Plot

A box plot splits the data set into quartiles. The body of the box plot consists of a "box", which goes from the first quartile (Q1) to the third quartile (Q3). Box plots have two types of orientations:

- Horizontal
- Vertical

In case of vertical orientation, a horizontal line is drawn at the Q2, the median of the data set. The *whiskers* are straight lines extending from the ends of the box to the maximum and minimum values. The lower whisker goes from Q1 to the smallest non-outlier in the data set, and the upper whisker goes from Q3 to the largest non-outlier. *Quartiles* separate the original set of data into four equal parts. Each of these parts contains one-fourth of the data. Quartiles are percentiles that divide the data into fourths.

- The first quartile Q_1 is the middle of lower half of the data. One-fourth of the data lies below the first quartile and three-fourths lies above
- The second quartile is also called median of the entire data set
- The third quartile is the middle of the upper half of the data. Three-fourths of data lies below the third quartile and one-fourth lies above.

Outliers are the data points which are either much higher or much lower than all of the other values.

The training set of the above 30 images are furthermore used to plot BOXPLOTS as shown below:

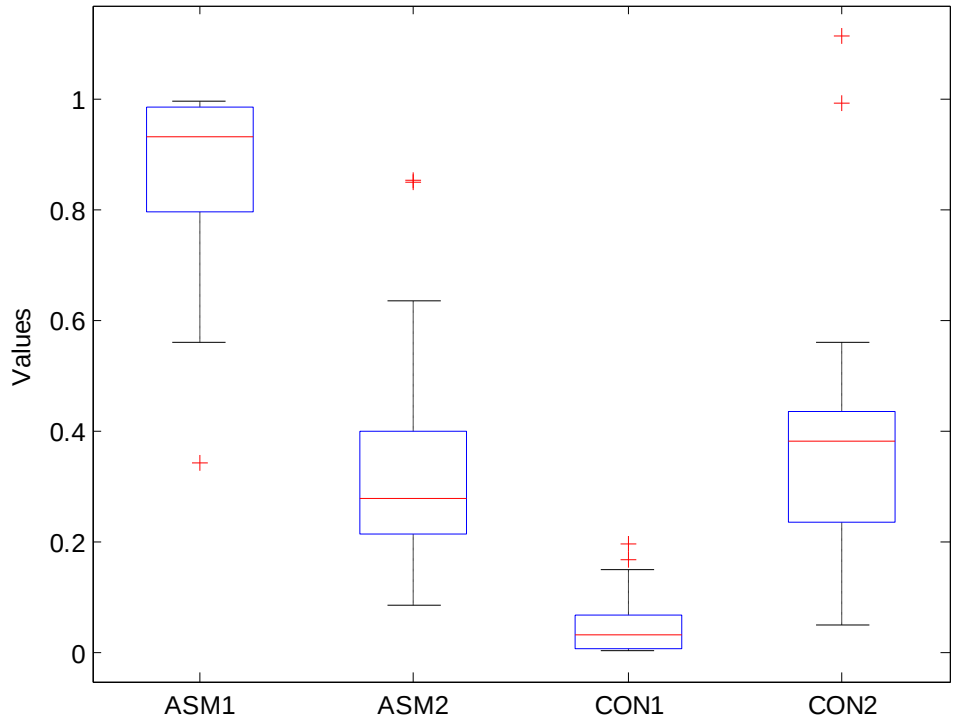

Figure 5.12 Box Plot for ASM and CON values

The above Box plot shows that ASM1 (water) and ASM2 (urban area) have different ranges so they can be used to discriminate between water and urban area. The minimum value of ASM1 is 0.3421 and maximum is 0.9935. The inter quartile range is 0.1717, Q1 is 0.8131 and Q3 is 0.9848. The red line shows median value of 0.92975. Similarly, the values of all the box plots are shown in table 5.31.

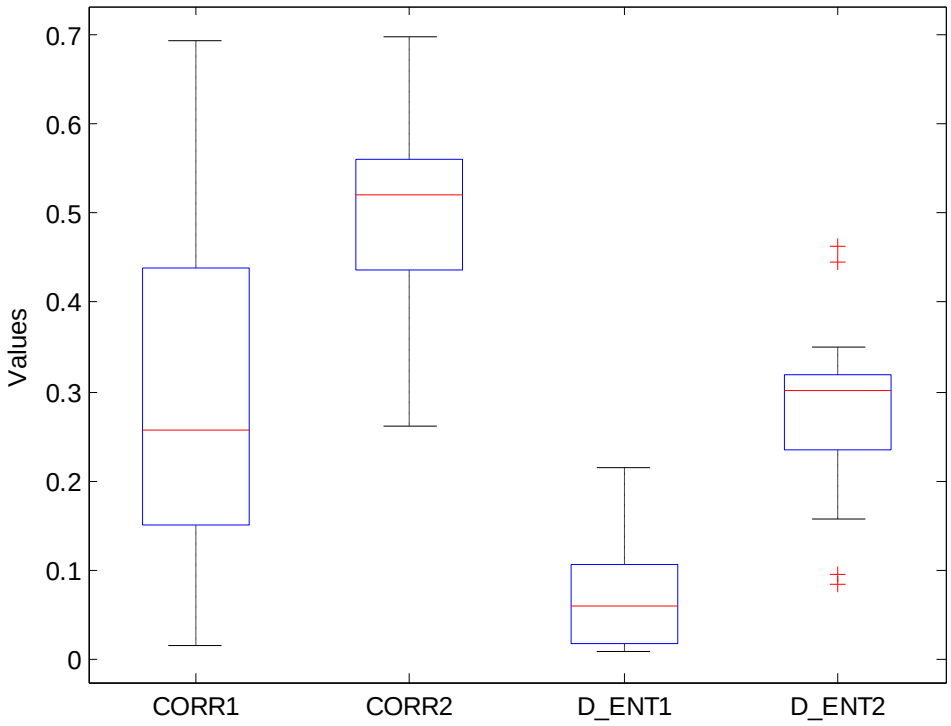

Figure 5.13 Box Plot of CORR and D_ENT values

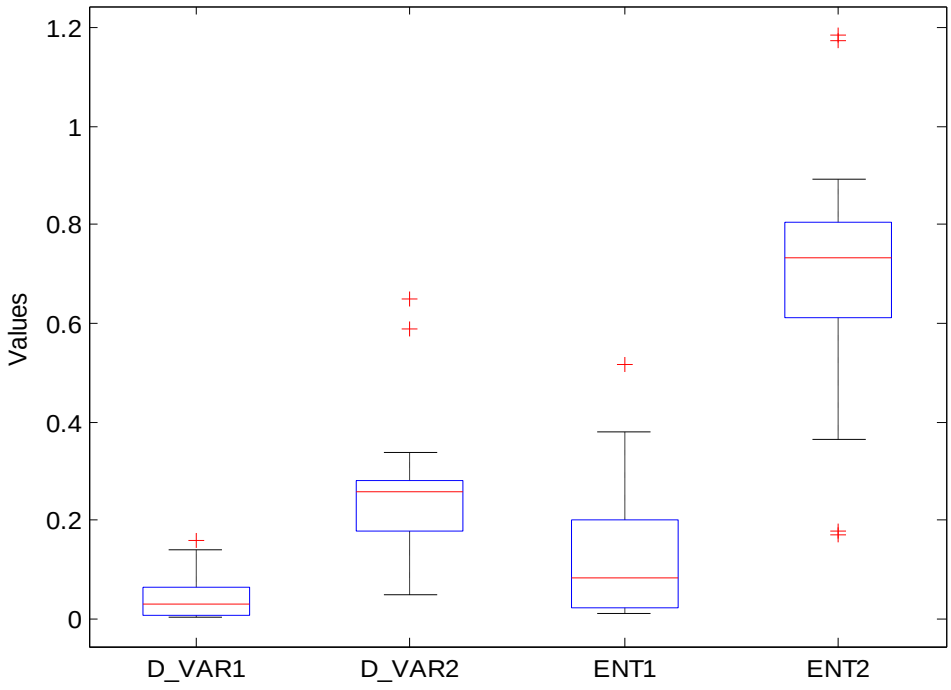

Figure 5.14 Box Plot of D_VAR and ENTROPY values

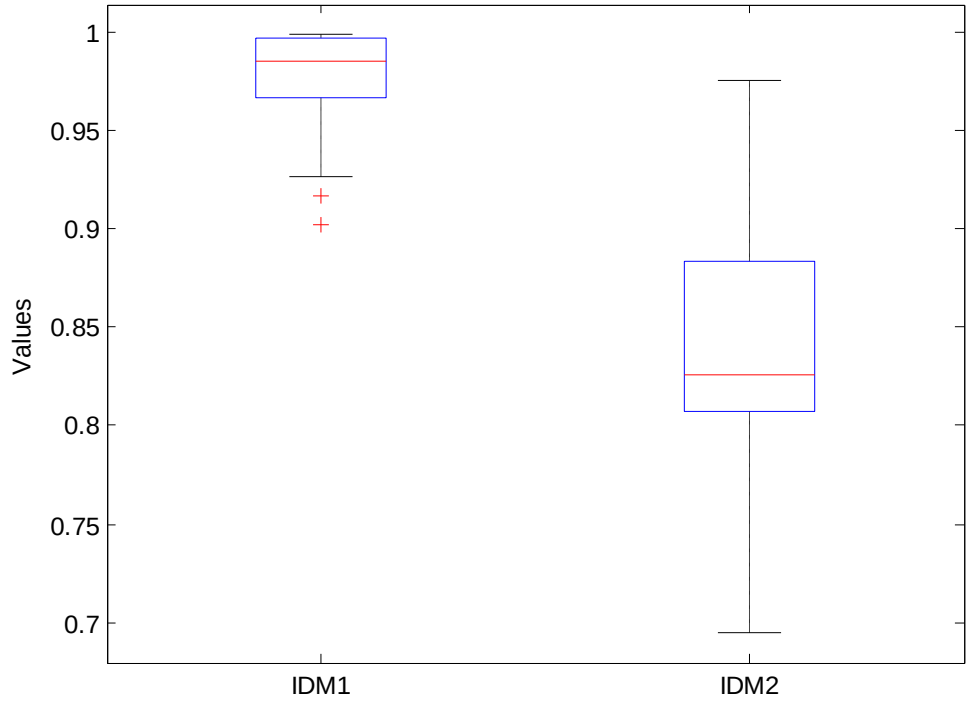

Figure 5.15 Box Plot of IDM values

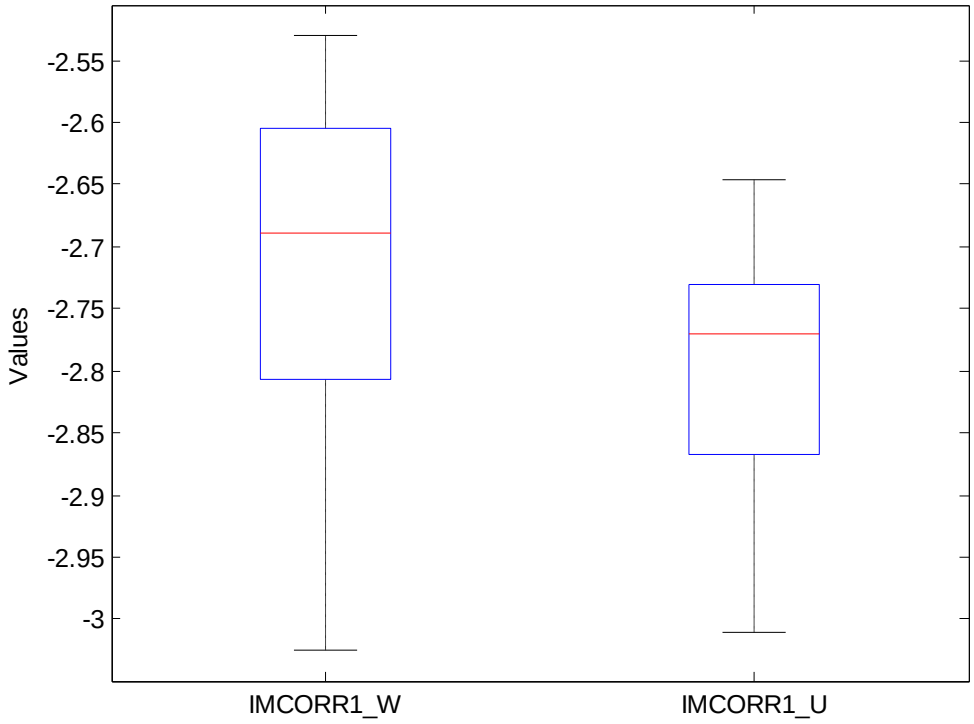

Figure 5.16 Box Plot of IMCORR1 values

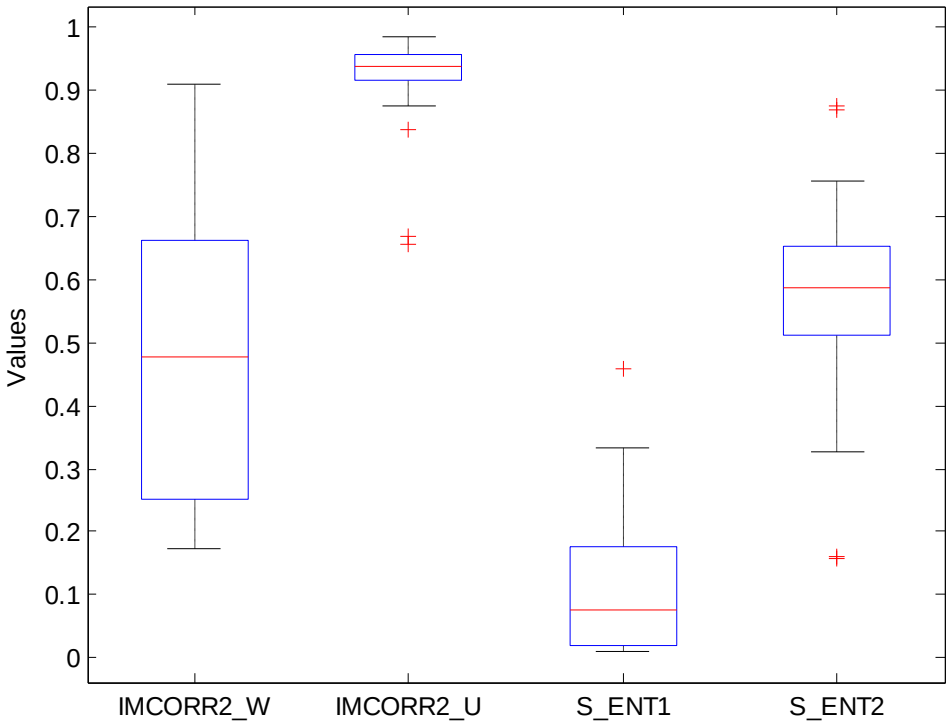

Figure 5.17 Box Plot of IMCORR2 and S_ENT values

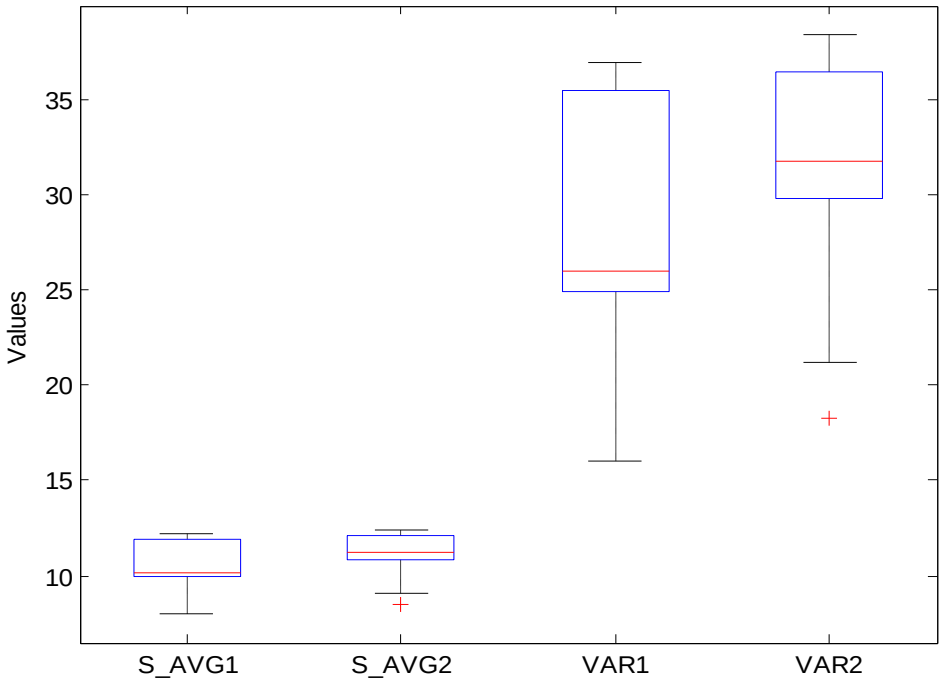

Figure 5.18 Box Plot of S_AVG and VARIANCE values

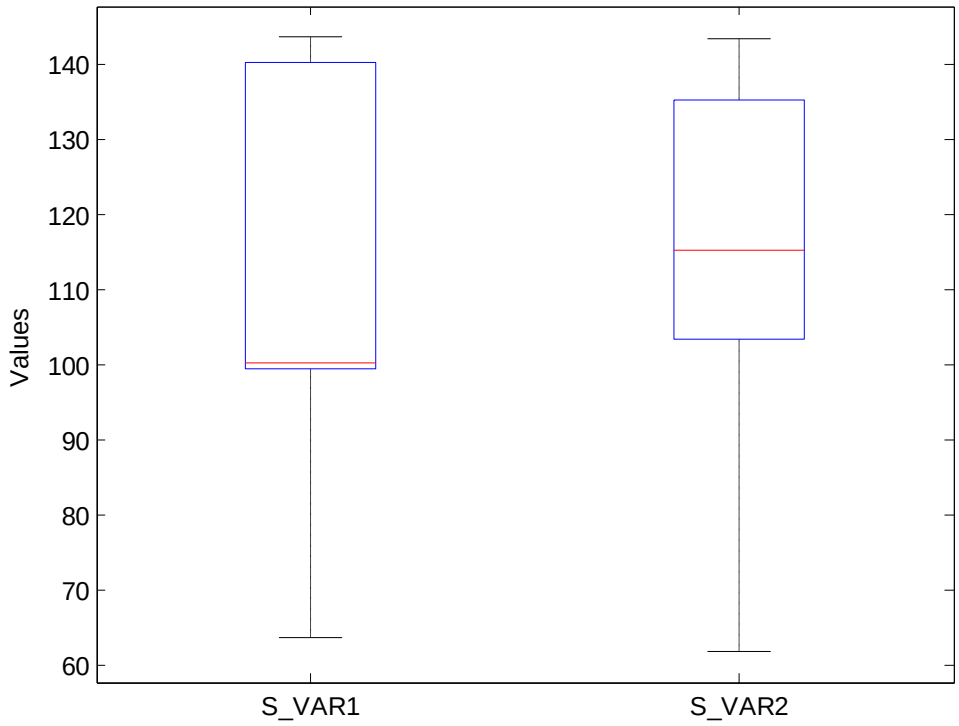

Figure 5.19 Box Plot of S_VARIANCE values

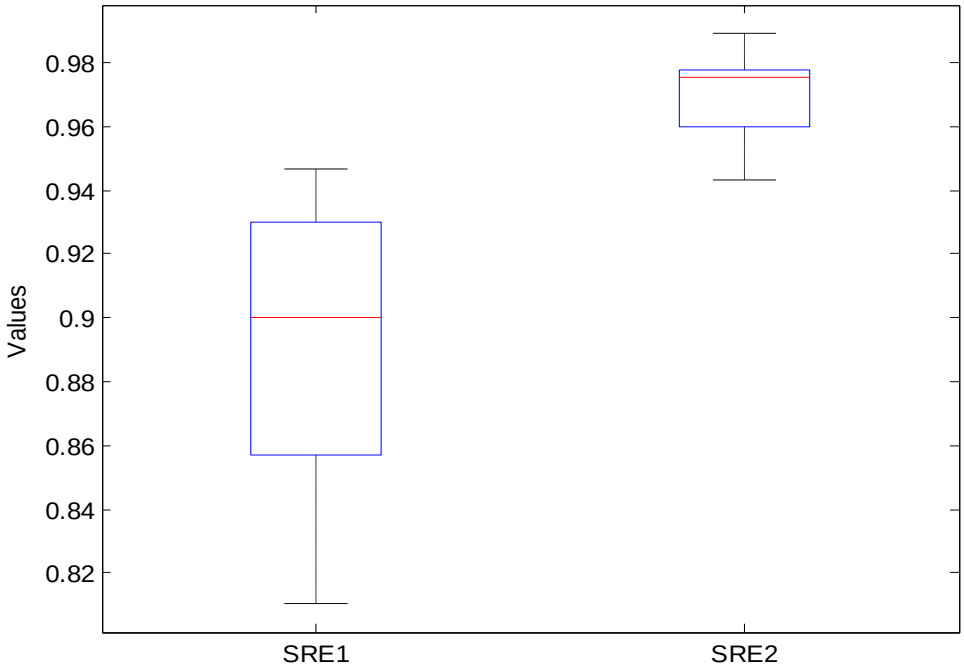

Figure 5.20 Box Plot of SRE values

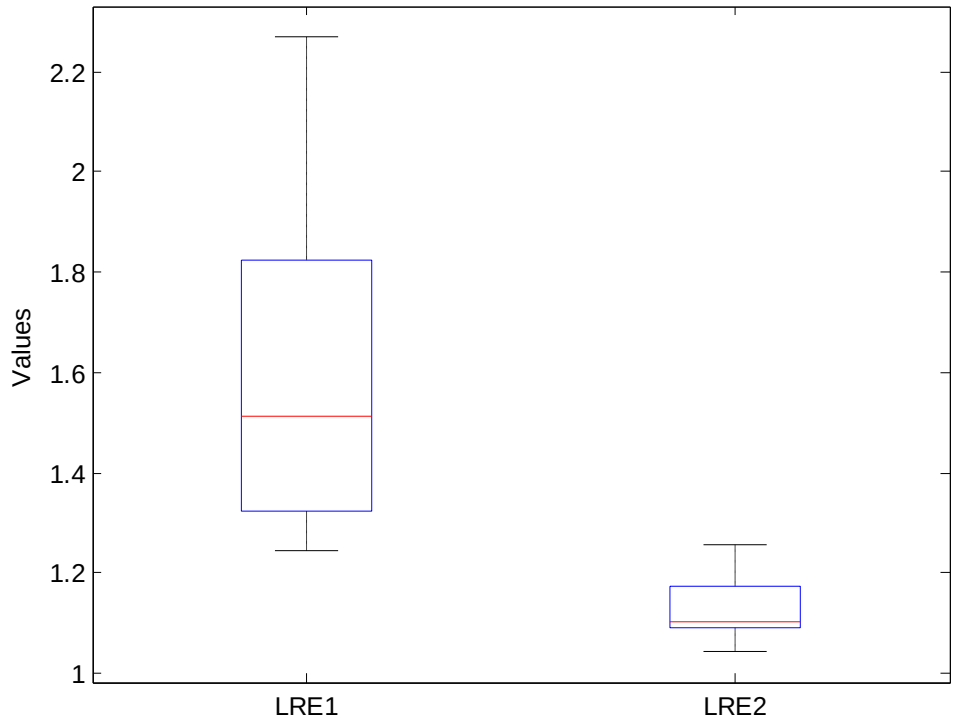

Figure 5.21 Box Plot of LRE values

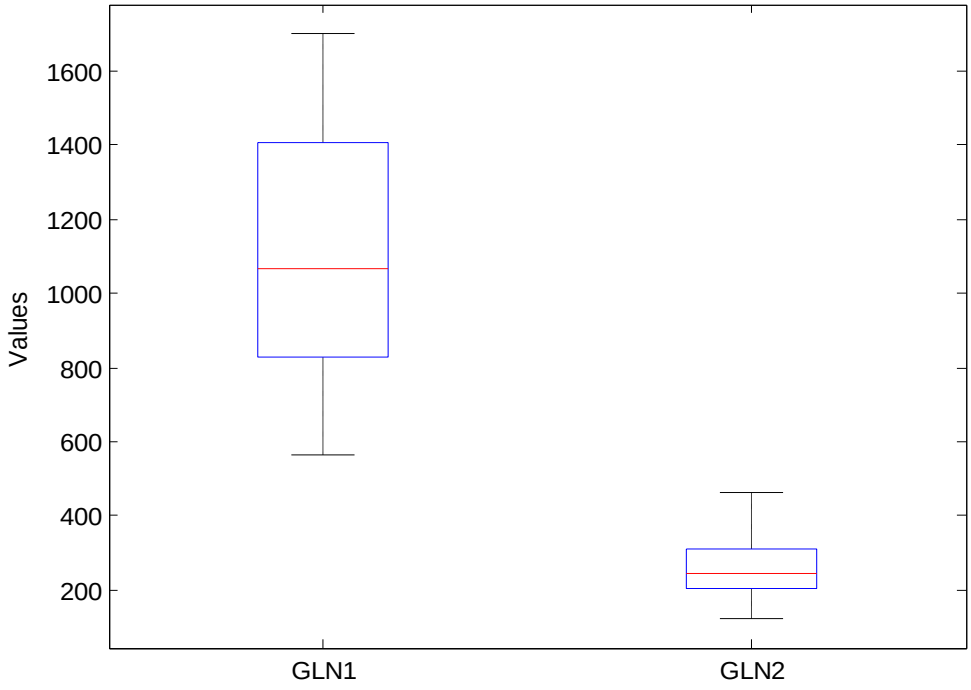

Figure 5.22 Box Plot of GLN values

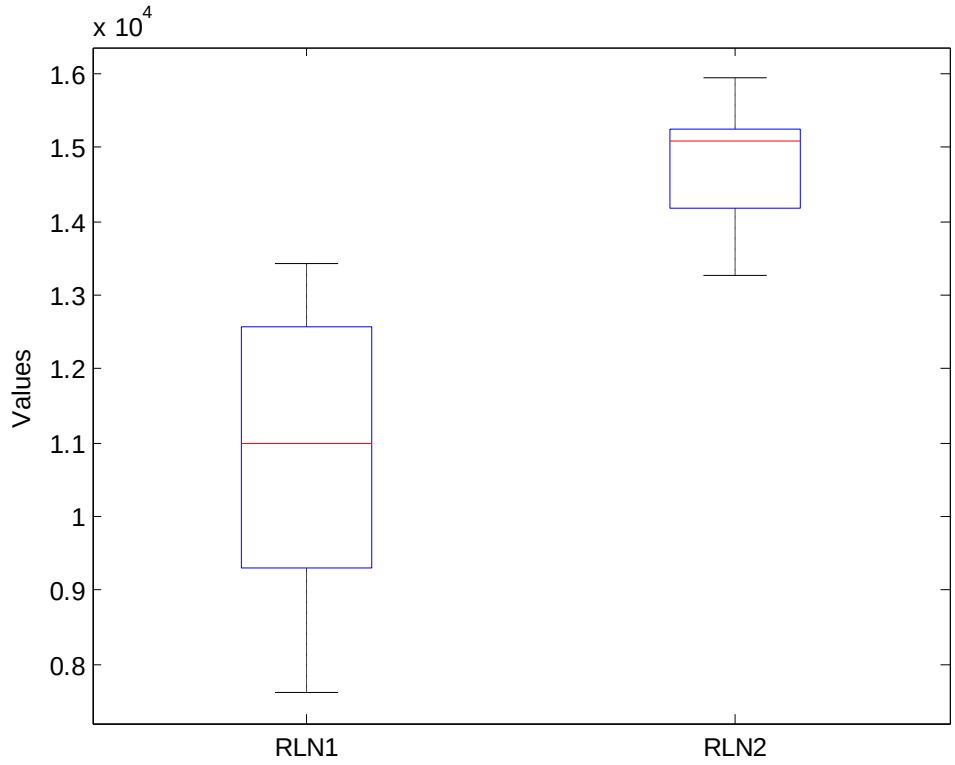

Figure 5.23 Box Plot of RLN values

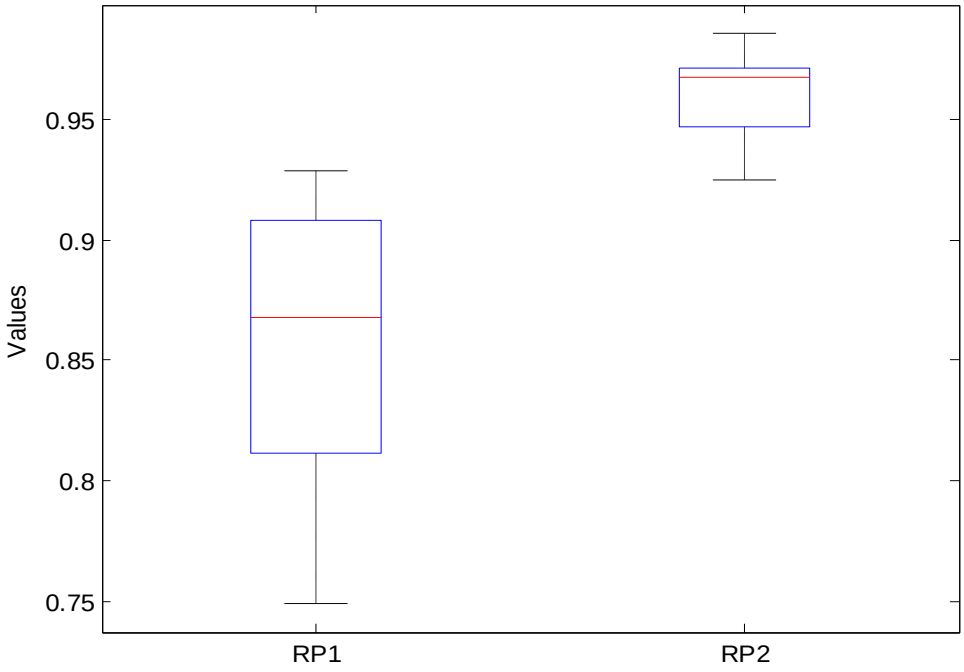

Figure 5.24 Box plot of RP values

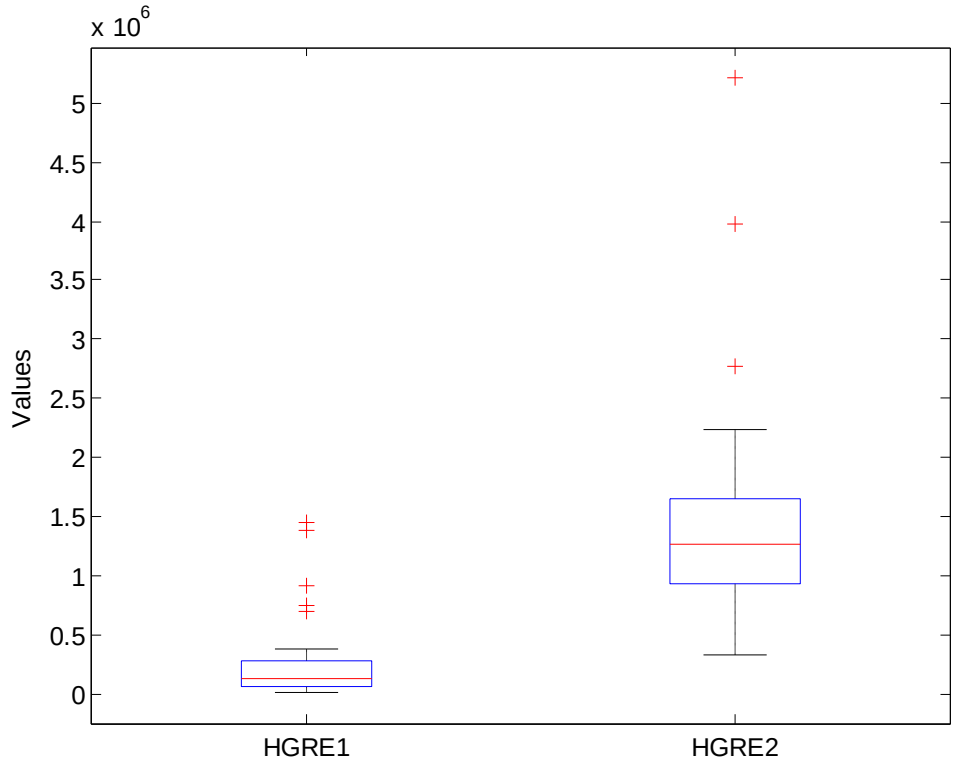

Figure 5.25 Box plot of HGRE values

BOXPLOTS of the training data for water and urban area coverage are as shown above. On the basis of box plots, we can find out which texture measure being computed is of our concern. For example, in the very first box plot, the ASM1 (ASM of water training data) is non-overlapping with ASM2 (ASM of building training data). So ASM is the measure which can be used further for our analysis. In this way, we find out all the non overlapping texture measures and found out the following:

1. ASM
2. CONTRAST
3. DIFF_ENTROPY
4. DIFF_VARIANCE
5. ENTROPY
6. IDM
7. INFO_MEAS_CORR2
8. SUM_ENTROPY
9. SRE
10. LRE

11. GLN
12. RLN
13. RP
14. HGRE

So the above fourteen texture measures are the ones distinguishing between water and building data.

Now, since we have found out 14 texture parameters out of 30, we can test the new images on the basis of only these 14 parameters. The range of respective parameters is found from box plots, which in turn, are used in the program. In this way, each new image which had to be tested was being given as input to the code and we got the results. The table showing the range of each value is as shown below:

Table 5.31 Statistical values of different parameters used in box plots

	ASM1	ASM2	CON1	CON2	D_ENT1	D_ENT2
Min	0.3421	0.0845	0.0034	0.0495	0.0092	0.0853
Q_1	0.81308	0.21568	0.00705	0.2502	0.01823	0.24405
Median	0.92975	0.27745	0.03115	0.3797	0.0602	0.3008
Q_3	0.98483	0.39998	0.0665	0.43145	0.1061	0.31705
Max	0.9935	0.8505	0.1966	1.1125	0.2152	0.4635
IQR	0.17175	0.1843	0.05945	0.18125	0.08788	0.073

	D_VAR1	D_VAR2	ENT1	ENT2	IDM1	IDM2
Min	0.0034	0.0483	0.0113	0.1724	0.9017	0.695
Q_1	0.00715	0.18838	0.02245	0.61263	0.9668	0.80743
Median	0.03105	0.25935	0.08375	0.7335	0.98445	0.82625
Q_3	0.0636	0.27923	0.1862	0.7983	0.99648	0.87813
Max	0.1583	0.6512	0.5162	1.1854	0.9985	0.9753
IQR	0.05645	0.09085	0.16375	0.18568	0.02968	0.0707

	IMCORR2_W	IMCORR2_U	S_ENT1	S_ENT2	SRE1	SRE2
Min	0.1723	0.6559	0.0103	0.1575	0.8104	0.9432
Q_1	0.2559	0.9164	0.02038	0.51155	0.85943	0.9625
Median	0.4786	0.937	0.0759	0.58725	0.9003	0.9757
Q_3	0.6431	0.954225	0.16143	0.64645	0.93008	0.9781
Max	0.908	0.9846	0.457	0.874	0.9466	0.9893
IQR	0.3872	0.037825	0.14105	0.1349	0.07065	0.0156

	LRE1	LRE2	GLN1	GLN2	RP1	RP2
Min	1.2454	1.0443	565.433	123.771	0.7493	0.925
Q_1	1.32273	1.09183	828.758	210.852	0.81473	0.95025
Median	1.5141	1.10335	1066.69	243.602	0.8675	0.96755
Q_3	1.80225	1.16355	1384.81	306.263	0.9082	0.9709
Max	2.2694	1.2576	1699.2	462.442	0.9287	0.9856
IQR	0.47953	0.07172	556.054	95.4111	0.09348	0.02065

	RLN1	RLN2	HGRE1	HGRE2
Min	7621.36	13252.7	19270.419	338562.85
Q_1	9407.71	14324.5	68792.273	953783.08
Median	10997.6	15098.4	132857.26	1269076.8
Q_3	12552.5	15245.1	272973.42	1649186.8
Max	13427.4	15940.5	1460932.8	5209877.7
IQR	3144.74	920.624	204181.15	695403.71

The range of each feature is from Q1 to Q3, where Q1 is the first quartile and Q3 is third quartile.

5.5 DISCRIMINATIVE POWER DISTANCE

The discriminative power distance is used to discriminate between two sets on the basis of distance. The formula for discriminative power distance is

$$d = \frac{\mu_1 - \mu_2}{\sqrt{{\sigma_1}^2 + {\sigma_2}^2}}$$

where subscript 1 is for water and subscript 2 is for land. Therefore, μ_1 is the mean of water and μ_2 is mean of urban area coverage and ${\sigma_1}^2$ and ${\sigma_2}^2$ are the respective variances of water and urban area coverage. We have calculated the distance d for all the 20 parameters as shown in table below.

Table 5.32 Discriminative Power Distance of Texture Parameters

PARAMETER	DISTANCE
GLN	2.469271
Sum_Entropy	2.261134
Entropy	2.146954
ASM	2.1366
RLN	1.994265
Diff_Entropy	1.97033
Info_meas_corr2	1.877758
IDM	1.862296
RP	1.765168
SRE	1.763112
Diff_Variance	1.539321
LRE	1.469181
Contrast	1.397311
HGRE	1.12538
Correlation	0.9703
Info_meas_corr1	0.459697
LGRE	0.447214
Variance	0.336431
Sum_Average	0.282659
Sum_Variance	0.012493

From the table, it is clear that GLN is having the highest distance and thus, is highly discriminative parameter. Finally, we reduced the number of parameters on the basis of above table by taking parameters having values more than d=1.5. So, we have the following reduced number of features as

1. GLN
2. SUM ENTROPY
3. ENTROPY
4. ASM
5. RLN
6. DIFF_ENTROPY
7. IMCORR2
8. IDM
9. RP
10. SRE

5.6 DIMENSION REDUCTION BY CORRELATION COEFFICIENT

To further reduce the dimension of the required number of features, we have found out Pearson's correlation coefficient of all the texture features for both water and urban area coverage as shown in the table below.

Table 5.33 Correlation Coefficient values for water

	GLN	S_ENT	ENTROPY	ASM	RLN	D_ENT	IMCORR2	IDM	RP	SRE
GLN	1	-0.1286	-0.13091732	0.12049	-0.737	-0.1526	-0.13004603	0.14419	-0.7461	-0.7463
S_ENT	-0.1286	1	0.99959847	-0.9958	-0.1138	0.96301	0.938867971	-0.9741	-0.1042	-0.1094
ENTROPY	-0.1309	0.9996	1	-0.9958	-0.1054	0.96877	0.938255265	-0.9801	-0.0962	-0.1014
ASM	0.12049	-0.9958	-0.99575731	1	0.11498	-0.948	-0.90495723	0.97275	0.10585	0.11066
RLN	-0.737	-0.1138	-0.10535412	0.11498	1	-0.0319	-0.1187316	0.04477	0.99776	0.99728
D_ENT	-0.1526	0.96301	0.968767029	-0.948	-0.0319	1	0.953531621	-0.9869	-0.0262	-0.0317
IMCORR2	-0.13	0.93887	0.938255265	-0.905	-0.1187	0.95353	1	-0.9122	-0.1098	-0.1163
IDM	0.14419	-0.9741	-0.98013538	0.97275	0.04477	-0.9869	-0.91217999	1	0.03972	0.04442
RP	-0.7461	-0.1042	-0.0962338	0.10585	0.99776	-0.0262	-0.1097742	0.03972	1	0.99983
SRE	-0.7463	-0.1094	-0.10139354	0.11066	0.99728	-0.0317	-0.11633993	0.04442	0.99983	1

Table 5.34 Correlation Coefficient values for urban area

	GLN	S_ENT	ENTROPY	ASM	RLN	D_ENT	IMCORR2	IDM	RP	SRE
GLN	1	-0.9774	-0.95404229	0.94494	-0.767	-0.8718	-0.888568	0.84361	-0.7709	-0.77
S_ENT	-0.9774	1	0.987847111	-0.9707	0.79198	0.92693	0.8980247	-0.8987	0.79598	0.79625
ENTROPY	-0.954	0.98785	1	-0.9558	0.81965	0.96505	0.8507368	-0.9471	0.82165	0.822
ASM	0.94494	-0.9707	-0.95582036	1	-0.8767	-0.9345	-0.928917	0.9132	-0.8812	-0.8811
RLN	-0.767	0.79198	0.819646143	-0.8767	1	0.89695	0.7409361	-0.9057	0.99975	0.99976
D_ENT	-0.8718	0.92693	0.965046098	-0.9345	0.89695	1	0.8105242	-0.9907	0.89792	0.89843
IMCORR2	-0.8886	0.89802	0.850736797	-0.9289	0.74094	0.81052	1	-0.7551	0.74963	0.74942
IDM	0.84361	-0.8987	-0.94712267	0.9132	-0.9057	-0.9907	-0.755088	1	-0.9046	-0.905
RP	-0.7709	0.79598	0.82165284	-0.8812	0.99975	0.89792	0.749633	-0.9046	1	0.99987
SRE	-0.77	0.79625	0.821999672	-0.8811	0.99976	0.89843	0.749419	-0.905	0.99987	1

5.7 DISCUSSION

The tables 5.1 to 5.13 show the GLCM parameters of water, table 5.14 to 5.26 show the same features for urban area. Similarly, tables 5.27 and 5.28 show GLRLM features of water and urban area respectively. As shown in these tables the range of all the features is varying. These features are then plotted in box plots to find out if a given feature is discriminative in nature. From the box plots, we have reduced the 20 features to 14 features. The range of variation of these 14 features for both water and urban area coverage are shown in table 5.31. Then on the basis of distance d, we further reduced the number of features to 10. The correlation between these features is then calculated and ultimately we have reduced the feature set to just 5 features. We have analysed that features like GLN, Sum Entropy, RLN, ASM and Info_meas_corr2 are having highest discriminative distance and are least correlated as shown in tables above. Then, we have calculated the sensitivity, specificity and accuracy to evaluate the proposed set of features for classification.

Table 5.35 Evaluation of Classification Accuracy

	Is it a water image?		
Did the test indicate the presence of water?		**Yes**	**No**
	Yes	True Positive (TP)	False Positive (FP) Image doesn't contain water but test indicates that it is water
	No	False Negative (FN) Image is of water but test says it is not	True Negative (TN)

On the basis of this formalism, following terms are used to indicate the quality of the classification.

- **SENSITIVITY or TRUE POSITIVE FRACTION (TPF)**
  It is the ratio of number of correct positive assumptions to the number of truly positive cases.

$$TPF = \frac{TP}{TP + FN}$$

- **SPECIFICITY or TRUE NEGATIVE FRACTION (TNF)**

  It is the ratio of number of correct negative cases to truly negative cases.

$$TNF = \frac{TN}{TN + FP}$$

- **ACCURACY**

  It is defined as ratio of number of correct cases to total number of cases.

$$ACCURACY = \frac{TP + TN}{TP + TN + FP + FN}$$

Based upon the above terms, the classification efficiency of the proposed method is evaluated as shown in table below.

TP	FP	FN	TN	SENSITIVITY	SPECIFICITY	ACCURACY
9	0	1	10	90%	100%	95%

Thus, the proposed system has a sensitivity of 90% which means the system recognizes 90% of all the images containing water i.e. 9 out of every 10 images.

The specificity of 100% means that system is very specific in identifying water images. Finally, the proposed system is 95% accurate.

Chapter 6
CONCLUSIONS AND FUTURE SCOPE

We have studied 30 images for 20 texture features. We have analysed these features and found the 5 highly discriminative features by using box plots, discriminative power distance and Pearson's coefficient of correlation. The final five features are

- GLN (Gray Level Non-Uniformity) from GLRLM
- Sum Entropy from GLCM
- ASM (Angular Second Moment) from GLCM
- RLN (Run Length Non-Uniformity) from GLRLM
- Information measure of correlation 2 from GLCM

Finally, we have evaluated the performance of these features on the test images and found that sensitivity is 90%, specificity is 100% and the accuracy for the classification has been 95%. So, we proposed a classification system for SAR images based on highly discriminative texture features.

In future, this work can be extended in using

- Fuzzy logic and Artificial Neural Networks for better classification.
- Number of test images can be increased for better accuracy.
- Dimension reduction can also be done using Principal Component Analysis.

REFERENCES

[1] Y.K.Chan and V.C.Koo, "An Introduction to Synthetic Aperture Radar", *Progress In Electromagnetic Research B*, Vol. 2, pp 27–60, 2008.

[2] R.M.Haralick, K.Shanmugam and H. Dinstein, "Textural Features for Image Classification", *IEEE Transactions on Systems, Man and Cybernetics*, Vol. No. 3, pp. 610 – 621, 1973.

[3] H.H.Loh, J.G.Leu and R.C.Luo, "The Analysis of Natural Textures Using Run Length Features," *IEEE Transactions on Industrial Electronics*, Vol. No. 35, pp. 323-328, 1988.

[4] Chung-Ming Wu, Yung-Chang Chen and Kai-Sheng Hsieh, "Texture Features for Classification of Ultrasonic Liver Images," *IEEE Transactions on Medical Imaging*, Vol. No. 11, pp. 141-152, 1992

[5] D.Patel, I.Hannah and E.R.Davies, "Texture Analysis for Foreign Object Detection Using a Single Layer Neural Network," *IEEE International Conference on Neural Networks*, Vol. No. 7, pp. 4265-4268, 1994.

[6] A.H.S.Solberg and A.K.Jain, "A Study of the Invariance Properties of Textural Features in SAR Images," *International Geoscience and Remote Sensing Symposium, IGARSS '95*, Vol. No. 1, pp. 670-672, 1995.

[7] A.H.Mir, M.Hanmandlu and S.N.Tandon, "Texture Analysis of CT Images*," IEEE Engineering in Medicine and Biology Magazine*, Vol. No.14, pp 781-786, 1995.

[8] L.Ma, T.Tan, Y.Wang and D.Zhang, "Personal Identification Based on Iris Texture Analysis," *IEEE Transactions on Pattern Analysis and Machine Intelligence*, Vol. No. 25, pp. 1519-1533, 2003.

[9] A.Abhyankar and S.Schuckers, "Fingerprint Liveness Detection using Local Ridge Frequencies and Multiresolution Texture Analysis Techniques," *IEEE International Conference on Image Processing*, pp. 321-324, 2006.

[10] N.Agani, S.A.R.Abu-Bakar & S.H.Sheikh Salleh, "Application of Texture Analysis in Echocardiography Images for Myocardial Infarction Tissue," *Journal Technology*, 46(D), pp. 61-76, 2007.

[11] F.Zhang, Y.Shao, W.Tian and S.Wang, "Oil Spill Identification Based on Textural Information of SAR Image," *IEEE International Geoscience and Remote Sensing Symposium IGARSS 2008*, Vol. No. 4, pp. 1308-1311, 2008

[12] V.V.Chamundeeswari, D.Singh, and K.Singh, "An Analysis of Texture Measures in PCA-Based Unsupervised Classification of SAR Images," *IEEE Geoscience and Remote Sensing Letters*, Vol. No. 6, pp. 214-218, 2009.

[13] Y.Cai and J.Chong, "Parameter Assessment for Texture Feature Quality evaluation in SAR ocean image," *2nd Asian-Pacific Conference on Synthetic Aperture Radar, APSAR 2009*, pp. 852-855, 2009.

[14] A.Kourgli, A. Belhadj-Aissa and Y. Oukil, "SAR Image Classification Using Textural Modeling," *Radar Conference-Surveillance for a Safer World*, pp. 1-6, 2009.